PROFITS, PANDEMICS, AND LOCKDOWN EFFECTIVENESS IN NURSING HOME NETWORKS

Roland Pongou
Dept. of Economics, University of Ottawa

Ghislain Junior Sidie
Dept. of Economics, University of Ottawa

Guy Tchuente
School of Economics, University of Kent

Jean-Baptiste Tondji
Dept. of Economics, University of Texas Rio Grande Valley

NIESR Discussion Paper No. 540
15th September 2022

About the National Institute of Economic and Social Research

The National Institute of Economic and Social Research is Britain's longest established independent research institute, founded in 1938. The vision of our founders was to carry out research to improve understanding of the economic and social forces that affect people's lives, and the ways in which policy can bring about change. Over eighty years later, this remains central to NIESR's ethos. We continue to apply our expertise in both quantitative and qualitative methods and our understanding of economic and social issues to current debates and to influence policy. The Institute is independent of all party-political interests.

National Institute of Economic and Social Research
2 Dean Trench St
London SW1P 3HE
T: +44 (0)20 7222 7665
E: enquiries@niesr.ac.uk
www.niesr.ac.uk
Registered charity no. 306083

This paper was first published in September 2022

Competing Interest Statement: The views expressed in this paper are based on research and are not attributed to the organizations to which the researchers are affiliated. There are no conflicts of interest. The usual disclaimer applies.

Profits, Pandemics, and Lockdown Effectiveness in Nursing Home Networks

Guy Tchuente, Roland Pongou, Ghislain Junior Sidie, and Jean-Baptiste Tondji

Abstract

How do pandemics affect for-profit and not-for-profit organizations differently? To address this question, we analyse optimal lockdowns in a two-sector continuous-time individual-based mean-field epidemiological model. We uncover a unique solution that depends on network structure, lockdown effectiveness, and the planner's tolerable infection incidence. Using unique data on nursing home networks in the United States, we calibrate the model and jointly quantify state-level lockdown effectiveness and preference for enforcing stringent containment strategies during the COVID-19 pandemic. We also empirically validate simulation results derived from the theoretical analyses. We find that for-profit nursing homes experience higher COVID-19 death rates than not-for-profit nursing homes. In addition, this differential health effect increases with lockdown effectiveness.

Classification: D85, E61, H12, I18, J14

Keywords: Pandemics, Profits, Social networks, Lockdown effectiveness, Nursing Homes

Profits, Pandemics, and Lockdown Effectiveness in Nursing Home Networks

Roland Pongou[1*], Ghislain Junior Sidie[1*], Guy Tchuente[2*] and Jean-Baptiste Tondji[3*]

[1]Dept. of Economics, University of Ottawa.
[2]School of Economics, University of Kent.
[3]Dept. of Economics, University of Texas Rio Grande Valley.

[*]Corresponding author(s). E-mail(s): rpongou@uottawa.ca; gsidi040@uottawa.ca; g.tchuente@kent.ac.uk; jeanbaptiste.tondji@utrgv.edu;

Abstract

How do pandemics affect for-profit and not-for-profit organizations differently? To address this question, we analyze optimal lockdowns in a two-sector continuous-time individual-based mean-field epidemiological model. We uncover a unique solution that depends on network structure, lockdown effectiveness, and the planner's tolerable infection incidence. Using unique data on nursing home networks in the United States, we calibrate the model and jointly quantify state-level lockdown effectiveness and preference for enforcing stringent containment strategies during the COVID-19 pandemic. We also empirically validate simulation results derived from the theoretical analyses. We find that for-profit nursing homes experience higher COVID-19 death rates than not-for-profit nursing homes. In addition, this differential health effect increases with lockdown effectiveness.

Keywords: Pandemics, Profits, Social networks, Lockdown effectiveness, Nursing Homes

JEL Classification: D85 , E61 , H12 , I18 , J14

1 Introduction

In a pandemic, governments face the difficult problem of selecting optimal intervention strategies to cope with the adverse effects of the health crisis. These decisions are challenging because more stringent measures generally result in economic contraction, while laissez-faire policies likely lead to a high death toll. Motivated by this dilemma, we consider the problem of designing lockdown interventions that optimize the tradeoff between fatalities due to virus spread and economic costs in a pandemic that spreads through networks of physical contacts. We are particularly interested in the distributional effects of such interventions across economic sectors, and how these effects interact with lockdown effectiveness. To address these questions, we develop an economic model of optimal lockdown. Using unique data on nursing home networks in the United States, we calibrate the model to quantify lockdown effectiveness and state-level preference for prioritizing health over wealth during the COVID-19 pandemic. Some of these nursing homes operate on a for-profit basis, while others do not. We analyze how the for-profit status of a nursing home affects death rate and how this interacts with lockdown effectiveness.

The COVID-19 pandemic has severely affected individuals and households worldwide. As of May 20, 2022, the World Health Organization reported more than 521 million confirmed cases of COVID-19 and over 6 million COVID-19 deaths globally (WHO, 2022). The scientific and medical communities agree that individuals over the age of 65 and those who suffer comorbidities have experienced the highest risk of mortality due to COVID-19 (Dessie & Zewotir, 2021; Fallon, Dukelow, Kennelly, & O'Neill, 2020; Makris, 2021). In developed countries, old age individuals are more likely to reside in nursing homes, and these facilities have borne the burden of COVID-19 mortality. Indeed, as of June 1, 2021, nearly one-third of U.S. COVID-19 deaths were linked to nursing homes (Conlen et al., 2021); also, residents of nursing homes represented 81% of all reported COVID-19 deaths in Canada and more than 50% in Sweden (Akhtar-Danesh, Baumann, Crea-Arsenio, & Antonipillai, 2022); and as of June 30, 2021, residents of nursing homes and long-term care facilities accounted for 74% of total COVID-19 deaths in Australia (Dykgraaf et al., 2021).[1]

Considering these realities, public and scientific discussions have generated interests among researchers and policymakers worldwide, with the goal of dissecting the associations between nursing homes' characteristics and COVID-19 outcomes, including infections and mortality. Addressing these issues is essential in implementing sustainable and resilient strategies for future pandemics since recent forecasts project that the population of nursing homes will rise

[1]For additional statistics on nursing homes' characteristics and COVID-19 fatalities, see, e.g., Giri, Chenn, and Romero-Ortuno (2021), Bach-Mortensen, Verboom, Movsisyan, and Degli Esposti (2021), Ioannidis, Axfors, and Contopoulos-Ioannidis (2021), Dykgraaf et al. (2021), Akhtar-Danesh et al. (2022), and the International Long-Term Care Policy Network report (Comas-Herrera et al., 2020) which provides updated international data on deaths attributed to COVID-19 among people living in care homes at https://ltccovid.org/questions/2-02/.

over time. For example, by 2035, one out of three U.S. households will be headed by an individual aged 65 or older (JCHS, 2016), and the share of the U.S. population older than age 85 will increase to about 3 percent by 2035 and to 4 percent by the mid-2040s (Favreault & Johnson, 2021). In some European countries, the demand for older care is expected to grow by up to 127% by 2050 (Giri et al., 2021; O'Neill et al., 2020).

In this paper, to analyze how COVID-19 outcomes differ for for-profit (FP) and not-for-profit (NFP) nursing homes, we use tools from optimal control theory to address the problem of designing an optimal non-pharmaceutical planning strategy that limits the number of fatalities due to a pandemic until a vaccine is fully developed. In particular, we consider a two-sector version of the controlled epidemiological N-SIRD (Susceptible, Infected, Recovered, Deceased) individual-based model (Pongou, Tchuente, & Tondji, 2022b) that takes into account the network structure of the population and the effect of government intervention policies. This approach enables integrating features such as the impact of lockdown and containment strategies. In our planning problem, the lockdown strategy is designed to account for the fact that not-for-profit nursing homes earn zero profits whereas for-profit nursing homes seek to maximize profits. We undertake a quantitative analysis of optimal lockdown policy in this framework.[2] Focusing on the long-term care markets and choosing parameters in line with early COVID-19 pandemic, we analyze the role of lockdown effectiveness in setting optimal confinement strategies during a pandemic. Using simulation-based and empirical evaluations based on unique data on U.S. nursing home networks[3], we show that U.S state governors response policies combined with state-level lockdown effectiveness contribute significantly to the dynamics of COVID-19 outcomes in U.S. nursing homes.[4]

We now briefly present our two-sector N-SIRD model with lockdown and the planning problem. The lockdown effectiveness parameter ($\theta \in [0,1]$) describes how effectively the lockdown policy reduces contagion. The latter assumption is an important departure from Pongou et al. (2022b) who assume that the lockdown fully reduces the contagion (i.e., $\theta = 1$). Allowing θ to be different from 1 is consistent with the early studies by Acemoglu, Chernozhukov, Werning, and Whinston (2021), Alvarez, Argente, and Lippi (2021), and Fajgelbaum, Khandelwal, Kim, Mantovani, and Schaal (2021) who evaluate the benefits of lockdown strategies on virus spread during the COVID-19

---

[2]We view a "lockdown policy" as a collection of costly preventive interventions that reduce social and work interactions. In addition to social distancing policies, a lockdown in nursing homes includes visitation restrictions imposed on visitors and non-essential health care personnel; such restrictions may not apply to compassionate care situations, such as an end-of-life situation as enforced by the U.S. Centers for Medicare & Medicaid Services from May 13, 2020, to September 17, 2020.

[3]Data on nursing home networks were collected by the researchers of the "Protect Nursing Homes" project hosted by Yale University; networks are built using smartphone data (Chen, Chevalier, & Long, 2021).

[4]Early studies also show that demographic and geographic characteristics explain differences in COVID-19 outcomes between countries and cities. For a cross-country comparison, we refer to Assob-Nguedia, Dongo, and Nguimkeu (2020) and Nguimkeu and Tadadjeu (2021) and the references therein.

pandemic. Additionally, in contrast to Pongou et al. (2022b), we split the population into two sectors or groups based on one key variable—nursing home ownership. In this regard, our work is related to recent studies that investigate the role of individual characteristics such as age on pandemic fatalities in epidemiological models (see, e.g., Gollier (2020), Acemoglu et al. (2021), and the references therein). Contrary to these previous works and more in line with Fajgelbaum et al. (2021), we provide a simulation-based estimation of the lockdown effectiveness in a network-based epidemiological model. Moreover, we study the effect of planners' tolerable infection incidence on the lockdown effectiveness during a pandemic. As such, we differ from Fajgelbaum et al. (2021) who evaluate the effects of optimal lockdown on mobility and trade in Seoul, Daegu, and New York City. We also differ by our research question, which is to analyze how COVID-19 outcomes depend on the for-profit status of a nursing home and how this effect varies with lockdown effectiveness.

To solve the tradeoff problem faced by the social planner, we first characterize the disease dynamics in our two-sector N-SIRD epidemiological model and obtain a unique solution under classical conditions. Proposition 1 shows that the rates of infection, recovery, and death at any given time are functions of the lockdown variable, the lockdown effectiveness, the initial network of contacts that captures social structure, and the epidemiological parameters. Second, we derive the planner's problem using optimal control theory, and we discuss conditions guaranteeing the uniqueness and multiplicity of solutions. Each feasible solution depends on the lockdown effectiveness, the infection incidence level tolerated by the social planner, and the prevailing network of physical interactions that characterize the population. Applying our theory to nursing homes, Proposition 2 shows that the optimal lockdown decreases with lockdown effectiveness for NFP nursing homes. However, as we illustrate in Remark 1, the relationship between our optimal lockdown policy and lockdown effectiveness in FP nursing homes is ambiguous. We provide an in-depth exploration of this association using simulations and empirical analysis as described below.

Using simulations that rely on parameters based on the early period of the COVID-19 pandemic and data on U.S. nursing home networks (Chen et al., 2021), we conduct some comparative statics analyses of our theoretical findings. For illustration, we consider a sample of nursing homes in Florida. Our results in Fig. 2 confirm the predictions of Proposition 2, and they show that for any given level of lockdown effectiveness, the size of lockdown is larger in NFP nursing homes than in FP homes, independently of the governor's tolerable infection incidence level. Additionally, the average lockdown probability seems to increase with lockdown effectiveness in FP nursing homes in Florida. However, the optimal lockdown dynamics in a random small-world network (Watts & Strogatz, 1998) that we display in Fig. 3 show that the monotonic relationship between optimal lockdown and lockdown effectiveness in FP nursing homes can be overturned, which supports our analysis in Remark 1.

In line with Pongou et al. (2022b), a higher tolerable infection incidence level results in less stringent lockdown and containment policies in FP nursing homes. As illustrated in Fig. A3, these policies translate into higher infections at the early stage of the pandemic, with FP nursing homes experiencing more infections than NFP nursing homes when the lockdown effectiveness is sufficiently high. We confirm these results using simulations on the random small-world network, finding that the death differential between FP and NFP nursing homes increases with lockdown effectiveness. The simulation results in Fig. A5 show that the economic costs of lockdown are largely carried by NFP nursing homes in Florida, whatever the degree of lockdown effectiveness. However, the economic costs increase with lockdown effectiveness in FP nursing homes. All of these simulation results indicate that lockdown effectiveness can be essential in explaining differences in pandemic fatalities between FP and NFP nursing homes.

We calibrate relevant parameters of our two-sector N-SIRD model and test our theoretical predictions using the unique U.S. nursing home networks data provided by Chen et al. (2021). Our calibration approach allows us to jointly estimate the value of the tolerable COVID-19 infection incidence level (ι) and the lockdown effectiveness (θ) for 40 U.S. states. The parameter ι estimates the U.S. state government's tolerable COVID-19 infection incidence, which by assumption represents the level at which the governor trades population health for short-term wealth. As such, a higher value of ι describes a less stringent containment strategy similar to a laissez-faire policy (Gollier, 2020) and indicating the behavior of a wealth-leaning social planner. The parameter θ estimates the state's preparedness for an effective lockdown strategy. In other words, θ represents the extent to which a lockdown strategy can effectively curb the diffusion of the virus.

Based on a simulated minimum distance estimator (e.g., Gertler and Waldman (1992), and Forneron and Ng (2018)), our calibration-estimated results show a great deal of variation in ι and θ across U.S. states. Our analysis suggests that variation in lockdown effectiveness can be explained by state-level differences in demographic and political characteristics. These factors include policy responses during the COVID-19 pandemic, the party affiliation of the governor, the approval rate of the governor, the state's OxCGRT indexes (Hale et al., 2021), the state's geographic location, the state GDP growth, the distribution of nursing homes' ownership in the state, and the number of COVID-19 deaths in the state. We use these variations to test some theoretical hypotheses of the model.[5]

Using regression-based analyses, we find that higher lockdown effectiveness increases the difference in COVID-19 death count between FP and NFP nursing homes. Also, the results suggest that governors in U.S. states with higher lockdown effectiveness tend to prefer less stringent lockdown and containment strategies to mitigate the pandemic, resulting in higher mortality in the long

[5]We retrieved data on U.S. governor approval for mandated COVID-19 policies on April 29, 2022, from the COVID STATES PROJECT accessible at https://lazerlab.shinyapps.io/Behaviors_During_COVID/. Our findings complement other studies showing an association between the political affiliation of a U.S. state's governor and COVID-19 fatalities (e.g., Neelon, Mutiso, Mueller, Pearce, and Benjamin-Neelon (2021), Baccini and Brodeur (2021), and Pongou et al. (2022b).

run. Additionally, states with a high proportion of FP nursing homes experience more deaths. Also, nursing homes that are more central in the network registered more COVID-19 mortality. Our results are robust when controlling for an array of nursing home and U.S. state-level characteristics, such as overall nursing home quality, county socioeconomic status, the OxCGRT indexes that capture government responses during the COVID-19 pandemic, and county fixed effects. Interestingly, our empirical results suggest that the difference in COVID-19 deaths between FP and NFP nursing homes is more pronounced in U.S. states with higher effective lockdown and containment strategies. The death differential is virtually similar in U.S. states with less effective containment measures; these are states with a low level of lockdown effectiveness.

Our paper contributes to the literature that combines epidemiology and economics to address various issues. The epidemiological framework that we use to model the planning problem is a continuous-time individual-based mean-field model which belongs to the class of theoretical approaches for epidemic modeling on undirected heterogeneous networks; Pastor-Satorras, Castellano, Van Mieghem, and Vespignani (2015) provide a review of these epidemiological models, and Boucekkine, Carvajal, Chakraborty, and Goenka (2021), Fajgelbaum et al. (2021), Debnam Guzman, Mabeu, and Pongou (2022), Pongou, Tchuente, and Tondji (2022a), Pongou et al. (2022b), Nganmeni, Pongou, Tchantcho, and Tondji (2022), and the references therein highlight the recent economic contributions to the COVID-19 pandemic.[6] Another contribution by Makris (2021) also extends the classical susceptible-infected-recovered (SIR) model by incorporating heterogeneity in infection-induced mortality rates at the population level. Makris assumes that two distinct groups (low-risk versus high-risk individuals) in the population face different epidemiological parameters in terms of infection and deaths and respond differently to social distancing policies enforced by the government. In this framework with endogenous social distancing behavior and imperfect control of human mobility, Makris analyzes, among others, the effects of pandemic mitigating responses on the COVID-19 outcomes and economic welfare in the United Kingdom. Although we share some policy tools (e..g., lockdown) in reducing the contagion as in these previous studies, we address a different issue with a distinct modeling approach.

We also contribute to the growing literature seeking to understand the results of poor pandemic outcomes in nursing homes. Giri et al. (2021) survey a set of full peer-reviewed articles available on the MEDLINE Ovid database from March 2020 to January 2021 and found that both internal and external factors contributed to an increased likelihood of COVID-19 outcomes in nursing homes. Internal factors include, among others, resident characteristics (e.g.,

[6] Our model also complements other economic studies that examine the diffusion of innovation or contagion in non-mean-field-based network models; see among others, Ballester, Calvó-Armengol, and Zenou (2006), Lloyd, Valeika, and Cintrón-Arias (2006), Young (2009), Young (2011), Pongou and Serrano (2013), Banerjee, Chandrasekhar, Duflo, and Jackson (2013), Buechel, Hellmann, and Klößner (2015), Battiston and Stanca (2015), Pongou and Tondji (2018), and Galeotti, Golub, and Goyal (2020).

comorbidities, mental state, malnutrition, race, and ethnicity), facility characteristics (e.g., number of beds occupied, the influx of staff and visitors, urban location, ownership status with FP nursing homes inducing high mortality, inadequate ventilation), and staffing (e.g., shortage, lack of skilled registered nurses). External factors include low policy priority of long-term care (especially in the U.S.), lack of personal protective equipment, and asymptomatic transmission of the SARS-CoV-2, the virus that causes COVID-19.

Similarly, Bach-Mortensen et al. (2021) also provides a systematic overview of peer-reviewed studies focusing on the relationship between long-term care home ownership and COVID-19 outbreaks, infections, and deaths. Bach-Mortensen et al. find that, although FP nursing homes are not consistently linked with a higher risk of COVID-19 outbreak, they experienced higher rates of COVID-19 cases and deaths. In line with Giri et al. (2021), factors affecting staffing, nursing home size, and resident characteristics contribute to adverse COVID-19 outcomes. Overall, these studies show that FP status and nursing home characteristics related to FP status are associated with worse COVID-19 fatalities.

In line with the previous review articles, Dykgraaf et al. (2021) also conduct a structured search of PubMed/Medline, Cochrane Library and Scopus (Health & Medicine, Elsevier) to November 24, 2020, and review 80 full-text eligible articles that investigate strategies that have prevented or mitigated SARS-CoV-2 transmission in long-term care. According to Dykgraaf et al. (2021), it is still early to detect which intervention was highly influential in mitigating the spread of SARS-CoV-2 in nursing homes. Nevertheless, current studies suggest that serial testing of residents and staff, especially when community prevalence is high, and workplace management approaches that provide incentives for staff training and retention with access to paid leave provisions are universal effective contagion strategies. Although the focus of our study is more in line with studies in Bach-Mortensen et al. (2021) that investigate the effects of nursing home ownership on the pandemic fatalities, our findings and those of the previous contributions could assist social planners in developing effective mitigation strategies against current and future pandemics. Our analysis differs from other studies in providing a micro-founded model to understand how nursing home ownership affects COVID-19 outcomes. We are also the first to document how differences in death between FP and NFP nursing homes depend on lockdown effectiveness. In addition, our empirical analysis exploits the network structure of our data to account for variables (e.g., network centrality index) not accounted for in other empirical studies that investigate the effect of nursing home ownership on COVID-19 outcomes.

The rest of this paper is organized as follows. In Section 2, we present our two-sector N-SIRD model with lockdown and the planning problem. Section 3 illustrates how lockdown effectiveness affects optimal lockdown and disease dynamics in nursing homes. Section 4 uses simulation results to describe the dynamic of epidemiological and economic outcomes in a network of nursing homes. Section 5 provides an empirical application of the theoretical model, and Section 6 concludes. The Appendices contain additional figures and tables.

2 Two-sector N-SIRD model with lockdown

We consider a combination of epidemiology and economics to address the problem of a social planner who wants to mitigate the health and economic burden of a viral respiratory infection affecting society in the absence of vaccines and treatments. The infection spreads through an undirected weighted and symmetric network of physical contacts that we denote by $\mathcal{M}$, with its adjacency matrix $(\mathcal{M}_{i,j})$, where $\mathcal{M}_{ij} = \mathcal{M}_{ji} \in [0, \infty)$ represents the *weight* or *intensity* at which individuals i and j are connected in $\mathcal{M}$, with $\mathcal{M}_{ij} = 0$ if $i = j$. Time t is continuous, $t \in [0, \infty)$, and contrary to the N-SIRD model with the lockdown by Pongou et al. (2022b), individuals are partitioned into two groups $g \in \{A, B\}$ with N^g initial members.[7] There is no vital dynamics so that the total population $N(t) = N^A(t) + N^B(t) = N \geq 1$ for all t. Individuals are subdivided into susceptible (S), infected (I), recovered (R), and deceased (D),

$$S(t) + I(t) + R(t) + D(t) = N.$$

At each period, each individual i is in each of the four different compartments with the following probabilities: $s_i = P(i \in S)$, $x_i = P(i \in I)$, $r_i = P(i \in R)$, and $d_i = P(i \in D)$, with $s_i + x_i + r_i + d_i = 1$.

Lockdown. We incorporate a lockdown variable to capture the fact that a social planner might decide to reduce the spread of the infection by enforcing a lockdown policy. This lockdown policy reduces the spread of infection by modifying the existing social network structure, $\mathcal{M}$. Let L denote the lockdown state that is controlled by the social planner, and $l_i = P(i \in L)$ denote the probability that a random individual i is sent into lockdown, with $l_i = 1$ designating full lockdown and $l_i = 0$ no lockdown. Following Acemoglu et al. (2021) and Alvarez et al. (2021), we assume that the lockdown is only partially effective in eliminating the transmission of the virus since some contacts will still happen in the population even under a full economic lockdown. Let θ denote a measure of the lockdown effectiveness. We can consider the latter as the rate at which lockdown effectively reduces the infection in the social network structure. By assumption, $\theta \in [0, 1]$.

Disease Dynamics. Susceptible individuals may become infected by coming into contact with infected individuals at a constant passing rate $\beta \in [0, 1]$. The probability of an individual i being infected is equal to the probability that they are susceptible (s_i) and not sent into full lockdown $(1 - \theta l_i > 0)$ multiplied by the probability that a neighbor j is infected $(x_j > 0)$ and is not sent into

[7] Following Gollier (2020) and Acemoglu et al. (2021), one can partition individuals into multiple groups, extending the N-SIRD model to a multi-group N-SIRD model with the lockdown. Given the complexity of the dynamics in mean-field network-based models, we keep our study in two sectors for simplicity and tractability.

full lockdown ($1-\theta l_j > 0$), scaled by the connection intensity between i and j ($\mathcal{M}_{ij} > 0$) and the contact rate β. The susceptible probability of an individual i evolves according to the differential equation:

$$\dot{s_i} = -\beta s_i(1-\theta l_i)\sum_{j\in N}[\mathcal{M}_{ij}(1-\theta l_j)x_j]. \tag{1}$$

Individuals move from susceptible to infected, then either recover at rate γ or die at rate κ, $\gamma, \kappa \in [0,1]$. The law of motion of the infective probability for individual i is then

$$\dot{x_i} = \beta s_i(1-\theta l_i)\sum_{j\in N}\mathcal{M}_{ij}(1-\theta l_j)x_j - (\gamma+\kappa)x_i. \tag{2}$$

For each $i \in N$, let $X_i = (x_i, s_i, r_i, d_i)^T$ denote agent i's health characteristics in the population group g, where T means "transpose." We summarize the laws of motion of the variables of interest given the lockdown profile $l = (l_i)_{i\in N}$ by the following nonlinear system of ordinary differential equations:

$$(\text{ODE}):\begin{cases}\dot{s_i} = -\beta s_i(1-\theta l_i)\sum_{j\in N}[\mathcal{M}_{ij}(1-\theta l_j)x_j]\\ \dot{x_i} = \beta s_i(1-\theta l_i)\sum_{j\in N}\mathcal{M}_{ij}(1-\theta l_j)x_j - (\gamma+\kappa)x_i\\ \dot{r_i} = \gamma x_i\\ \dot{d_i} = \kappa x_i\\ s_i + x_i + r_i + d_i = 1\end{cases}$$

where the initial value point $(x_i(0), s_i(0), r_i(0), d_i(0))$ is such that

$$x_i(0) \geq 0,\ s_i(0) \geq 0,\ r_i(0) \geq 0,\ d_i(0) \geq 0,\ \text{and}\ x_i(0)+s_i(0)+r_i(0)+d_i(0) = 1.$$

Proposition 1 demonstrates the existence of a solution for the system (ODE).

Proposition 1 *The system (ODE) admits a unique solution* $\mathcal{S}^* = \mathcal{S}^*(l, \mathcal{M}, \beta, \gamma, \kappa, \theta)$.

Proof Given that $s_i = 1 - x_i - r_i - d_i$, for each $i \in N$, we can rewrite (ODE) as:

$$(\text{ODE}):\begin{cases}\dot{s_i} = -\beta(1-x_i-r_i-d_i)(1-\theta l_i)\sum_{j\in N}[\mathcal{M}_{ij}(1-\theta l_j)x_j]\\ \dot{x_i} = \beta(1-x_i-r_i-d_i)(1-\theta l_i)\sum_{j\in N}[\mathcal{M}_{ij}(1-\theta l_j)x_j] - (\gamma+\kappa)x_i\\ \dot{r_i} = \gamma x_i\\ \dot{d_i} = \kappa x_i.\end{cases}$$

Consider $F_i(t,X_i) = (F_{i1}(t,X_i), F_{i2}(t,X_i), F_{i3}(t,X_i), F_{i4}(t,X_i))^T$, a vector-valued function, where

$$\begin{aligned}
F_{i1}(t,X_i) &= \beta(1-x_i-r_i-d_i)(1-\theta l_i)\sum_{j\in N}[\mathcal{M}_{ij}(1-\theta l_j)x_j] - (\gamma+\kappa)x_i \\
F_{i2}(t,X_i) &= -\beta(1-x_i-r_i-d_i)(1-\theta l_i)\sum_{j\in N}[\mathcal{M}_{ij}(1-\theta l_j)x_j] \\
F_{i3}(t,X_i) &= \gamma x_i \text{ and} \\
F_{i4}(t,X_i) &= \kappa x_i.
\end{aligned}$$

The function F_{ik} is a continuously differentiable function, for each $i \in N$ and $k \in \{1,2,3,4\}$. Consequently, the ODE admits a unique solution, $\mathcal{S}^*(l,\mathcal{M},\beta,\gamma,\kappa,\theta,X_0)$, thanks to the theorem of existence and uniqueness of a solution for first-order general ordinary differential equations, where $l = (l_i)_{i\in N} \in [0,1]^n$ is a vector of individual lockdown probabilities. □

We apply the system (ODE) on the COVID-19 dynamics in nursing homes in the United States (U.S.). Generally, nursing home services in the U.S. social care market (as in several other countries) are delivered by a combination of for-profit (FP), not-for-profit (NFP) and public providers. FP providers are commonly known as private adult social care firms operating on a for-profit basis, NFPs are known as providers registered not-for-profit or charitable organizations, and public providers are understood as those operated by central or local government.[8] Throughout, the group A (or FP) represents for-profit nursing homes and the group B (or NFP) consists of not-for-profit nursing homes, including public providers. The planning problem consists of choosing the optimal lockdown policy that will contain the contagion below a tolerable infection incidence threshold, $\iota \in [0,1]$, while minimizing the economic costs of lockdown for FP nursing homes while allowing NFP nursing homes to break-even.[9] A lockdown policy in a nursing home could include a combination of restrictions of family visits, interdiction on admitting new residents in the nursing home, and interdiction of transferring residents from hospitals or other care homes to the nursing home. Below, we formalize the planning problem.

The planning problem. Using the differential equation that describes the evolution of infection probability $\dot{x_i}$ in the system (ODE), the first objective of the planner is to select a lockdown policy $l = (l^A, l^B)$, where $l^A = (l_i)_{i\in A}$, $l^B = (l_i)_{i\in B}$, such that:

$$\dot{x_i} \equiv \dot{x_i}(l) \le \iota. \tag{3}$$

At any given period t, each nursing home i possesses a capital level k_i, and a labor supply h_i. Capital combines with labor to generate output, y_i, based on a production function: $y_i = y_i(k_i,h_i) = y_i(k_i,s_i,x_i,r_i,d_i,l_i)$. We assume that y_i is continuous and differentiable in each of its input variables. With the above information, nursing home i's surplus function, Π_i, is given as:

$$\Pi_i(k_i,h_i) = p_i y_i(k_i,h_i) - w_i h_i(s_i,x_i,r_i,d_i,l_i) \equiv \Pi_i(k_i,s_i,x_i,r_i,d_i,l_i). \tag{4}$$

[8]For additional information on nursing home ownership, see Bach-Mortensen et al. (2021).

[9]We refer to the work by Pongou et al. (2022b) for more intuitive explanations of this tradeoff between enforcing stringent mitigating strategies and short-term economic gains.

To minimize the economic costs of lockdown before the vaccine and cure, the planner wants all nursing homes to stay afloat and provide essential services to families and patients. Non-profit nursing homes should remain as close as possible to the pre-pandemic productivity levels, i.e.,

$$\Pi_i(k_i, s_i, x_i, r_i, d_i, l_i) = 0, \text{ for all } i \in N^B. \tag{5}$$

We assume that the function Π_i is jointly concave in the variables $(k_i, s_i, x_i, r_i, d_i, l_i)$ for all $i \in N$. The latter assumption is also guaranteed if we assume that the revenue function $p_i y_i$ (or simply the production function, y_i) is jointly concave in its variables, and the labor cost function $w_i h_i$ (or simply the labor supply, h_i) is jointly convex in its variables. Given the lockdown profile $l = (l^A, l^B) \in [0,1]^n$, and Eq.(5), the aggregate surplus is

$$W(k, s, x, r, d, l) = \sum_{i \in N^A} \Pi_i(k_i, s_i, x_i, r_i, d_i, l_i), \tag{6}$$

because following Eq. (5), for each $i \in N^B$, $\Pi_i = 0$. Using optimal control theory, we express the social planner's problem as:

$$\begin{array}{ll}
\underset{l=(l^A,l^B)}{\text{Maximize}} & \int\limits_0^\infty e^{-\delta t} \sum\limits_{i \in N^A} \{p_i y_i(k_i, h_i) - w_i h_i(s_i, x_i, r_i, d_i, l_i)\}\, dt \\
\text{subject to} & \dot{s_i} = -\beta s_i (1 - \theta l_i) \sum\limits_{j \in N} [\mathcal{M}_{ij}(1 - \theta l_j) x_j], \ i \in N \\
& \dot{x_i} = \beta s_i (1 - \theta l_i) \sum\limits_{j \in N} \mathcal{M}_{ij}(1 - \theta l_j) x_j - (\gamma + \kappa) x_i, \ i \in N \\
& \dot{r_i} = \gamma x_i, \ i \in N \\
& \dot{d_i} = \kappa x_i, \ i \in N \\
& s_i + x_i + r_i + d_i = 1, \ i \in N \\
& \dot{x_i} \leq \iota, \ i \in N \\
& p_i y_i(k_i, h_i) - w_i h_i(s_i, x_i, r_i, d_i, l_i) = 0 \text{ for all } i \in N^B, \\
& l_i(t) \in [0,1], \ i \in N, \text{ and } t, \\
& \text{and initial conditions } X(0),
\end{array} \tag{7}$$

where δ is the social planner's discount rate. Note that all state variables, s, x, r, and d in the problem (7) depend on the control (or lockdown) variable l. Since for each $i \in N$, $s_i = 1 - x_i - r_i - d_i$, in the system (ODE), we can rewrite the social planner's problem in (7) as:

$$
\begin{array}{ll}
\underset{l=(l^A,l^B)}{\text{Maximize}} & \int\limits_0^\infty e^{-\delta t} \sum\limits_{i\in N^A} \{p_i y_i(k_i,h_i) - w_i h_i(x_i,r_i,d_i,l_i)\}\, dt \\
\text{subject to} & \dot{x}_i = \beta(1-x_i-r_i-d_i)(1-\theta l_i) \sum\limits_{j\in N} \mathcal{M}_{ij}(1-\theta l_j)x_j - (\gamma+\kappa)x_i,\ i\in N \\
& \dot{r}_i = \gamma x_i,\ i\in N \\
& \dot{d}_i = \kappa x_i,\ i\in N \\
& \dot{x}_i \leq \iota,\ i\in N \\
& p_i y_i(k_i,h_i) - w_i h_i(x_i,r_i,d_i,l_i) = 0 \text{ for all } i\in N^B, \\
& l_i(t)\in[0,1],\ i\in N,\ \text{and } t, \\
& \text{and initial conditions } X(0).
\end{array} \tag{8}
$$

In the system (8), we denote

$$f_i(x_i,r_i,d_i,l_i) = \beta(1-x_i-r_i-d_i)(1-\theta l_i)\sum_{j\in N}\mathcal{M}_{ij}(1-\theta l_j)x_j - (\gamma+\kappa)x_i.$$

Then, $\dot{x}_i = f_i$. We assume that the control function $l_i : t \longrightarrow l_i(t) \in [0,1]$ is continuous (or piecewise-continuous) and differentiable. Given that the function Π_i is concave, it follows that Π_i and the objective function, $e^{-\delta t}W(k,x,r,d,l)$ in (8) are continuous and differentiable functions of their variables. Moreover, f_i and the right-hand sides of the laws of motion in (8) are all continuous and differentiable. The current Hamiltonian of the social planner's problem in the system (8) is:

$$\mathcal{H}_c(l,x,r,d,\mu^1,\mu^2,\mu^3) = \sum_{i\in N^A}\Pi_i(k_i,h_i)+\sum_{i\in N}\mu_i^1 f_i+\sum_{i\in N}\mu_i^2\gamma x_i+\sum_{i\in N}\mu_i^3\kappa x_i,$$

where μ_i^j $(j=1,2,3)$, for each $i\in N$, are costate variables. Given the constraints $\dot{x}_i\leq\iota$, $l_i(t)\in[0,1]$ for all $i\in N$, and $\Pi_i(k_i,h_i)=0$, for all $i\in N^B$, we can augment the current Hamiltonian $\mathcal{H}_c$ into the current Lagrangian function:

$$
\begin{aligned}
\mathcal{L}_c(l,x,r,d,\mu^1,\mu^2,\mu^3,\eta^1,\eta^2,\eta^3,\eta^4) &= \sum_{i\in N^A}\Pi_i(k_i,h_i)+\sum_{i\in N}\mu_i^1 f_i+\sum_{i\in N}\mu_i^2\gamma x_i \\
+\sum_{i\in N}\mu_i^3\kappa x_i + \sum_{i\in N}\eta_i^1(\iota-f_i) &+ \sum_{i\in N}\eta_i^2 l_i + \sum_{i\in N}\eta_i^3(1-l_i) + \sum_{i\in N^B}\eta_i^4\Pi_i(k_i,h_i)
\end{aligned}
$$

where the parameters η^j, $j=1,2,3,4$, are Lagrange multipliers. For any subset O of N, let $\mathbf{1}_O$ be the function defined on N by

$$\mathbf{1}_O(i) = \begin{cases} 1 & \text{if } i\in O \\ 0 & \text{if otherwise.} \end{cases}$$

We can rewrite $\mathcal{L}_c$ as:

$$\mathcal{L}_c(l, x, r, d, \mu^1, \mu^2, \mu^3, \eta^1, \eta^2, \eta^3, \eta^4) = \sum_{i \in N} \left(\mathbf{1}_{N^A}(i) + \eta_i^4 \left(1 - \mathbf{1}_{N^A}(i)\right)\right) \Pi_i(k_i, h_i)$$
$$+ \sum_{i \in N} (\mu_i^1 - \eta_i^1) f_i + \sum_{i \in N} \mu_i^2 \gamma x_i + \sum_{i \in N} \mu_i^3 \kappa x_i + \iota \sum_{i \in N} \eta_i^1 + \sum_{i \in N} \eta_i^2 l_i + \sum_{i \in N} \eta_i^3 \left(1 - l_i\right) \tag{9}$$

The first-order conditions for maximizing $\mathcal{L}_c$ call for, assuming interior solutions,

$$\frac{\partial \mathcal{L}_c}{\partial l_k} = 0, \; k \in N, \tag{10}$$

as well as for each $k \in N$:

$$\frac{\partial \mathcal{L}_c}{\partial \eta_k^1} = \iota - \dot{x_k} \geq 0, \qquad \eta_k^1 \geq 0, \qquad \eta_k^1 \frac{\partial \mathcal{L}_c}{\partial \eta_k^1} = \eta_k^1(\iota - \dot{x_k}) = 0, \tag{11}$$
$$\frac{\partial \mathcal{L}_c}{\partial \eta_k^2} = l_k \geq 0, \qquad \eta_k^2 \geq 0, \qquad \eta_k^2 \frac{\partial \mathcal{L}_c}{\partial \eta_k^2} = \eta_k^2 l_k = 0, \text{ and} \tag{12}$$
$$\frac{\partial \mathcal{L}_c}{\partial \eta_k^3} = 1 - l_k \geq 0, \qquad \eta_k^3 \geq 0, \qquad \eta_k^3 \frac{\partial \mathcal{L}_c}{\partial \eta_k^3} = \eta_k^3(1 - l_k) = 0, \tag{13}$$

and the break-even condition for NFP nursing homes:

$$\frac{\partial \mathcal{L}_c}{\partial \eta_i^4} = \Pi_i(k_i, h_i) = 0, \text{ for all } i \in N^B. \tag{14}$$

Finally, the other maximum-principle conditions that include the dynamics for state and co-state variables are, for $k \in N$:

$$\dot{x_k} = \frac{\partial \mathcal{L}_c}{\partial \mu_k^1} \qquad \dot{r_k} = \frac{\partial \mathcal{L}_c}{\partial \mu_k^2} \qquad \dot{d_k} = \frac{\partial \mathcal{L}_c}{\partial \mu_k^3} \tag{15}$$

$$\dot{\mu_k^1} = \delta \mu_k^1 - \frac{\partial \mathcal{L}_c}{\partial x_k} \qquad \dot{\mu_k^2} = \delta \mu_k^2 - \frac{\partial \mathcal{L}_c}{\partial r_k} \qquad \dot{\mu_k^3} = \delta \mu_k^3 - \frac{\partial \mathcal{L}_c}{\partial d_k} \tag{16}$$

Let denote by $\{l^*(t)\}_t$ an optimal path of the control variable, and an optimal path for state variables by $\{X_t^* = (x^*(t), r^*(t), d^*(t), s^*(t))\}_t$. We note that Eqs. (10)–(16) constitute a set of necessary conditions, which characterize the optimal solution of the optimal control problem under infinite time horizon. As it stands, Eqs. (10) and (16) do not allow us to solve the system of differential equations constituted by (10)–(16) since we only have an initial condition for X_t^*, namely $X^*(0) = X(0)$, and a complete solution of the system (8) requires two boundary conditions. Therefore, we need to find another boundary condition. Generally, to obtain the complete solution of the optimal control under infinite time horizon, the following conditions are required for the transversality condition at infinity:

$$\lim_{t\to\infty} \mu_k^1(t) \geq 0 \text{ and } \lim_{t\to\infty} \mu_k^1(t)x_k(t) = 0; \tag{17}$$

$$\lim_{t\to\infty} \mu_k^2(t) \geq 0 \text{ and } \lim_{t\to\infty} \mu_k^2(t)r_k(t) = 0; \tag{18}$$

$$\lim_{t\to\infty} \mu_k^3(t) \geq 0 \text{ and } \lim_{t\to\infty} \mu_k^3(t)d_k(t) = 0. \tag{19}$$

Let denote

$$\mathcal{H}_c^{max}(x, r, d, \mu^1, \mu^2, \mu^3, t) = \max_l \mathcal{H}_c(l, x, r, d, \mu^1, \mu^2, \mu^3, t). \tag{20}$$

By definition, each state variable x, r, or d is non-negative at each period t. Assume that given the list (μ^1, μ^2, μ^3) and t, the map $(x, r, d) \longrightarrow \mathcal{H}_c^{max}(x, r, d, \mu^1, \mu^2, \mu^3, t)$ is jointly concave in the variables (x, r, d). Then, if $\{l^*(t)\}_t$, $\{X_t^* = (x^*(t), r^*(t), d^*(t), s^*(t))\}_t$, and $\{(\mu^1(t), \mu^2(t), \mu^3(t))\}_t$ constitute a solution of the system comprised by (10)–(19), then the lockdown profile $\{l^*(t)\}_t$ is the solution of the social planner's problem in (8). In case the function $\mathcal{H}_c^{max}(x, r, d, \mu^1, \mu^2, \mu^3, t)$ is jointly strictly concave in the variables (x, r, d), then the optimal path $\{l^*(t)\}_t$ is unique. In Section 3, we use simulations to highlight the relationship between lockdown effectiveness and optimal lockdown in U.S. nursing homes.

3 Lockdown effectiveness and optimal lockdown

In this section, we use comparative statics simulation-based analysis to examine how lockdown effectiveness could affect lockdown and disease dynamics in nursing homes. First, to calibrate the model, we choose the parameters to match the data on U.S nursing homes from Chen et al. (2021).

Calibrating the production function. We consider the following functional forms for the labor function (h) and the production function (y):

$$h_i\left(s_i, x_i, r_i, d_i, l_i\right) = \left(1 + \chi_i^1 s_i r_i \left(1 - x_i\right)\left(1 - d_i\right)\right)\left(1 - \chi_i^2 \theta l_i\right), \tag{21}$$

$$y_i\left(k_i, s_i, x_i, r_i, d_i, l_i\right) = k_i^{\alpha_i} h_i^{1-\alpha_i}, \tag{22}$$

where $\chi_i^1 \in [0, 1]$ determines the direct effect on the rate of change in the labor supply when individual i is in one of the natural health compartments, S, I, R and D. The parameter $\chi_i^2 \in [0, 1]$ represents the direct effect on the labor supply which occurs when individual i is placed in lockdown, with this effect assumed to be non-positive. In Eq. (22), α_i is the elasticity of output with respect to the capital, and $1 - \alpha_i$ is the elasticity of output with respect to labor. The functions h_i in Eq. (21) and y_i in Eq. (22) satisfy the standard conditions mentioned in Section 2.

In what follows, we extend the theoretical derivation of the planning problem, which proves useful in our simulations. Recall that

$$f_i(x_i, r_i, d_i, l_i) = \beta(1 - x_i - r_i - d_i)(1 - \theta l_i) \sum_{j \neq i} [\mathcal{M}_{ij}(1 - \theta l_j)x_j] - (\gamma + \kappa)x_i.$$

Then,

$$\frac{\partial f_i}{\partial l_k} = \begin{cases} -\beta\theta(1 - x_i - r_i - d_i) \sum_{j \neq i} [\mathcal{M}_{ij}(1 - \theta l_j)x_j] & \text{if } k = i \\ -\beta\theta(1 - x_i - r_i - d_i)(1 - \theta l_i)\mathcal{M}_{ik}x_k & \text{if } k \neq i \end{cases}$$

$$\frac{\partial f_i}{\partial x_k} = \begin{cases} -\beta(1 - \theta l_i) \sum_{j \neq i} [\mathcal{M}_{ij}(1 - \theta l_j)x_j] - (\gamma + \kappa) & \text{if } k = i \\ \beta(1 - x_i - r_i - d_i)(1 - \theta l_i)(1 - \theta l_k)\mathcal{M}_{ik} & \text{if } k \neq i \end{cases}$$

$$\frac{\partial f_i}{\partial r_k} = \frac{\partial f_i}{\partial d_k} = \begin{cases} -\beta(1 - \theta l_i) \sum_{j \neq i} [\mathcal{M}_{ij}(1 - \theta l_j)x_j] & \text{if } k = i \\ 0 & \text{if } k \neq i. \end{cases}$$

We also recall that

$$\Pi_i(k_i, s_i, x_i, r_i, d_i, l_i) \equiv \Pi_i(k_i, x_i, r_i, d_i, l_i) = p_i y_i(k_i, x_i, r_i, d_i, l_i) - w_i h_i(x_i, r_i, d_i, l_i).$$

Therefore, for each i and k, and for each u in $\{x_k, r_k, d_k, l_k\}$, it holds that

$$\frac{\partial \Pi_i}{\partial u} = \begin{cases} p_i \frac{\partial y_i}{\partial u} - w_i \frac{\partial h_i}{\partial u} & \text{if } k = i \\ 0 & \text{if } k \neq i. \end{cases} \tag{23}$$

For each $k \in N$, we can write $\frac{\partial \mathcal{L}_c}{\partial l_k}$ as:

$$\begin{aligned} \frac{\partial \mathcal{L}_c}{\partial l_k} &= \sum_{i \in N} \left(\mathbf{1}_{N^A}(i) + \eta_i^4 \left(1 - \mathbf{1}_{N^A}(i)\right)\right) \frac{\partial \Pi_i}{\partial l_k} + \sum_{i \in N} (\mu_i^1 - \eta_i^1) \frac{\partial f_i}{\partial l_k} + \eta_k^2 - \eta_k^3 \\ &\overset{(23)}{=} \left(\mathbf{1}_{N^A}(k) + \eta_k^4 \left(1 - \mathbf{1}_{N^A}(k)\right)\right) \frac{\partial \Pi_k}{\partial l_k} + \sum_{i \in N} (\mu_i^1 - \eta_i^1) \frac{\partial f_i}{\partial l_k} + \eta_k^2 - \eta_k^3. \end{aligned}$$

Hence, using the first-order conditions in Eq. (10), Eq. (23) becomes:

$$\left(\mathbf{1}_{N^A}(k) + \eta_k^4 \left(1 - \mathbf{1}_{N^A}(k)\right)\right) \left(p_k \frac{\partial y_k}{\partial l_k} - w_k \frac{\partial h_k}{\partial l_k}\right) + \sum_{i \in N} (\mu_i^1 - \eta_i^1) \frac{\partial f_i}{\partial l_k} + \eta_k^2 - \eta_k^3 = 0. \tag{24}$$

Continuing our analysis of problem (8), we need to differentiate Eq. (24) with respect to time t. In line with the data of U.S. nursing home networks (Chen et al., 2021), we assume that the production function is Cobb-Douglas, and for simplification, we also assume that capital is constant over time, i.e., for each $i \in N$, $k_i := k_i(t) = K$, for all t. We also approximate labor supply as a linear function of lockdown as follow (for more details, see Section 4):

$$h_k = 1 - \theta l_k,\ k \in N. \tag{25}$$

Then,

$$y_k = K^\alpha (1 - \theta l_k)^{1-\alpha},\ k \in N,\ \alpha \in [0,1]. \tag{26}$$

Differentiating y_k and h_k with respect to l_k yield:

$$\frac{\partial y_k}{\partial l_k} = -(1-\alpha)\theta K^\alpha (1-\theta l_k)^{-\alpha} \text{ and } \frac{\partial h_k}{\partial l_k} = -\theta.$$

It follows that:

$$\frac{\partial^2 y_k}{\partial t \partial l_k} = -\alpha(1-\alpha)\theta^2 K^\alpha \dot{l_k}(1-\theta l_k)^{-\alpha-1} \text{ and } \frac{\partial^2 h_k}{\partial t \partial l_k} = 0.$$

For $k \neq i$, recall that $\frac{\partial f_i}{\partial l_k} = -\beta\theta(1 - x_i - r_i - d_i)(1-\theta l_i)\mathcal{M}_{ik} x_k$. Then,

$$\begin{aligned} \frac{\partial^2 f_i}{\partial t \partial l_k} &= \beta\theta(\dot{x}_i + \dot{r}_i + \dot{d}_i)(1-\theta l_i)\mathcal{M}_{ik} x_k + \beta\theta^2(1 - x_i - r_i - d_i)\dot{l_i}\mathcal{M}_{ik} x_k \\ &- \beta\theta\,(1 - x_i - r_i - d_i)\,(1-\theta l_i)\mathcal{M}_{ik} f_k. \end{aligned}$$

For $k = i$, we also have $\frac{\partial f_i}{\partial l_k} = -\beta\theta(1 - x_i - r_i - d_i)\sum_{j\neq i}[\mathcal{M}_{ij}(1-\theta l_j)x_j]$. Then,

$$\begin{aligned} \frac{\partial^2 f_i}{\partial t \partial l_i} &= \beta\theta(\dot{x}_i + \dot{r}_i + \dot{d}_i)\sum_{j\neq i}[\mathcal{M}_{ij}(1-\theta l_j)x_j] \\ &- \beta\theta\,(1 - x_i - r_i - d_i)\sum_{j\neq i}[(1-\theta l_j)f_j - \theta\dot{l_j}x_j]\mathcal{M}_{ij}. \end{aligned}$$

Differentiating Eq. (24) with respect to time t, assuming that prices p and w are time-invariant yield:

$$E_1 + \beta\theta\sum_{i\in N}\left(\mu_i^1 - \eta_i^1\right)\left(\delta_{ik}E_2 + (1-\delta_{ik})\mathcal{M}_{ik}E_3\right) + E_4 = 0, \tag{27}$$

where $\delta_{ik} = 1$ if $k = i$ and $\delta_{ik} = 0$ if $k \neq i$, and

$$E_1 = \left(\mathbf{1}_{N^A}(k) + \eta_k^4\,(1 - \mathbf{1}_{N^A}(k))\right)\left(-\alpha(1-\alpha)\theta^2 p_k K^\alpha \dot{l_k}(1-\theta l_k)^{-\alpha-1}\right)$$

$$E_2 = \left(\dot{x}_i + \dot{r}_i + \dot{d}_i\right)\sum_{j\neq i}[\mathcal{M}_{ij}(1-\theta l_j)x_j] - (1 - x_i - r_i - d_i)\sum_{j\neq i}[(1-\theta l_j)\dot{x}_j - \theta\dot{l_j}x_j]\mathcal{M}_{ij}$$

$$E_3 = \left(\dot{x}_i + \dot{r}_i + \dot{d}_i\right)(1-\theta l_i)x_k + \theta(1-x_i-r_i-d_i)\dot{l}_i x_k - (1-x_i-r_i-d_i)(1-\theta l_i)\dot{x}_k$$

$$E_4 = \sum_{i\in N}(\dot{\mu}_i^1 - \dot{\eta}_i^1)\frac{\partial f_i}{\partial l_k} + \dot{\eta}_k^2 - \dot{\eta}_k^3.$$

Using Eq. (27), we obtain an expression of $\dot{l}_k$ as follow:

$$\dot{l}_k = \frac{1}{\overline{E}_1}\left[\beta\theta\sum_{i\in N}\left(\mu_i^1 - \eta_i^1\right)\left(\delta_{ik}E_2 + (1-\delta_{ik})\mathcal{M}_{ik}E_3\right) + E_4\right], \text{ where} \quad (28)$$

$$\overline{E}_1 = \left(\mathbf{1}_{N^A}(k) + \eta_k^4\left(1-\mathbf{1}_{N^A}(k)\right)\right)\left(\alpha(1-\alpha)\theta^2 p_k K^\alpha (1-\theta l_k)^{-\alpha-1}\right).$$

Using the other conditions from Eq. (16) and using Eq. (23), we obtain:

$$\begin{aligned}\dot{\mu}_k^1 &= \delta\mu_k^1 - \frac{\partial\mathcal{L}_c}{\partial x_k}\\ &= \delta\mu_k^1 - \left(\mathbf{1}_{N^A}(k) + \eta_k^4\left(1-\mathbf{1}_{N^A}(k)\right)\right)\left(p_k\frac{\partial y_k}{\partial x_k} - w_k\frac{\partial h_k}{\partial x_k}\right) - \mu_k^2\gamma - \mu_k^3\kappa\\ &- \sum_{i\in N}(\mu_i^1 - \eta_i^1)\frac{\partial f_i}{\partial x_k}\end{aligned}$$

$$\begin{aligned}\dot{\mu}_k^2 &= \delta\mu_k^2 - \frac{\partial\mathcal{L}_c}{\partial r_k}\\ &= \delta\mu_k^2 - \left(\mathbf{1}_{N^A}(k) + \eta_k^4\left(1-\mathbf{1}_{N^A}(k)\right)\right)\left(p_k\frac{\partial y_k}{\partial r_k} - w_k\frac{\partial h_k}{\partial r_k}\right) - \sum_{i\in N}(\mu_i^1 - \eta_i^1)\frac{\partial f_i}{\partial r_k}\end{aligned}$$

$$\begin{aligned}\dot{\mu}_k^3 &= \delta\mu_k^3 - \frac{\partial\mathcal{L}_c}{\partial d_k}\\ &= \delta\mu_k^3 - \left(\mathbf{1}_{N^A}(k) + \eta_k^4\left(1-\mathbf{1}_{N^A}(k)\right)\right)\left(p_k\frac{\partial y_k}{\partial d_k} - w_k\frac{\partial h_k}{\partial d_k}\right) - \sum_{i\in N}(\mu_i^1 - \eta_i^1)\frac{\partial f_i}{\partial d_k}\end{aligned}$$

Finally, we can derive the derivatives of Lagrange multipliers with respect to time. Using Eqs. (11), (12), and (13), it follows that:

$$\eta_k^1(\iota - \dot{x}_k) = 0 \text{ implies } \dot{\eta}_k^1 = \frac{\ddot{x}_k}{\iota - \dot{x}_k}\eta_k^1, \quad (29)$$

$$\eta_k^2 l_k = 0 \text{ implies } \dot{\eta}_k^2 = -\frac{\dot{l}_k}{l_k}\eta_k^2, \text{ and} \quad (30)$$

$$\eta_k^3(1-l_k)=0 \text{ implies } \dot{\eta_k^3}=\frac{\dot{l_k}}{(1-l_k)}\eta_k^3. \quad (31)$$

Given the above specifications for the labor in Eq. (25), and the production function in Eq. (26), Proposition 2 provide a simple comparative static analysis between the lockdown and the lockdown effectiveness parameter θ for not-for-profit nursing homes.

Proposition 2 *The optimal lockdown decreases with lockdown effectiveness for not-for-profit nursing homes.*

Proof Let $k \in N$ be a NFP nursing home. Then $k \in N^B$, and $p_k y_k - w_k h_k = 0$. This implies $p_k K^\alpha (1-\theta l_k)^{1-\alpha} - w_k(1-\theta l_k) = 0$. Then, $l_k = \frac{1}{\theta}$ or $l_k = \frac{1}{\theta}\left[1-\left(\frac{p_k K^\alpha}{w_k}\right)^{\frac{1}{\alpha}}\right]$. For $\theta = 1$, we have $l_k = 1$ or $l_k = 1-\left(\frac{p_k K^\alpha}{w_k}\right)^{\frac{1}{\alpha}}$. We note that when the capital (K) and the output-price-wage ratio $(\frac{p_k}{w_k})$ are constant over time, the lockdown probability, l_k, is constant over time and it only depends on the lockdown effectiveness θ (given any value of α). When $K < \left(\frac{w_k}{p_k}\right)^{\frac{1}{\alpha}}$, then $1 > \left(\frac{p_k K^\alpha}{w_k}\right)^{\frac{1}{\alpha}}$, and $l_k > 0$. Also, we have $0 \le l_k \le 1$ if and only if $\frac{1-\theta}{K} \le \left(\frac{p_k}{w_k}\right)^{\frac{1}{\alpha}} < \frac{1}{K}$ or $\left(\frac{1-\theta}{K}\right)^\alpha \le \frac{p_k}{w_k} < \left(\frac{1}{K}\right)^\alpha$. It holds that $\frac{\partial l_k}{\partial \theta} = -\frac{1}{\theta^2} < 0$ or $\frac{\partial l_k}{\partial \theta} = -\frac{1}{\theta^2}\left[1-\left(\frac{p_k K^\alpha}{w_k}\right)^{\frac{1}{\alpha}}\right] \le 0$. $\square$

Remark 1 Using the above specifications on production functions, we note that the relationship between optimal lockdown and lockdown effectiveness for FP nursing homes is ambiguous. In fact, let k be a FP nursing home. Then, $k \in N^A$, and using equation (24), it holds that:

$$-(1-\alpha)\theta p_k K^\alpha (1-\theta l_k(\theta))^{-\alpha} + \theta w_k + \sum_{i\in N}(\mu_i^1 - \eta_i^1)\frac{\partial f_i}{\partial l_k} + \eta_k^2 - \eta_k^3 = 0, \quad (32)$$

where,

$$\frac{\partial f_i}{\partial l_k} = -\beta(1-x_i-r_i-d_i)\left[\delta_{ik}\sum_{j\ne i}\mathcal{M}_{ij}(\theta-\theta^2 l_j)x_j + (1-\delta_{ik})(\theta-\theta^2 l_i)\mathcal{M}_{ik}x_k\right].$$

Taking the derivative of Eq. (32) with respect to θ gives:

$$\begin{aligned}&-(1-\alpha)p_k K^\alpha(1-\theta l_k(\theta))^{-\alpha} - \alpha(1-\alpha)\theta p_k K^\alpha(l_k+\theta\frac{\partial l_k}{\partial\theta})(1-\theta l_k)^{-\alpha-1} + w_k + \\ &\sum_{i\in N}(\frac{\partial\mu_i^1}{\partial\theta} - \frac{\partial\eta_i^1}{\partial\theta})\frac{\partial f_i}{\partial l_k} + \sum_{i\in N}(\mu_i^1-\eta_i^1)\frac{\partial^2 f_i}{\partial\theta\partial l_k} + \frac{\partial\eta_k^2}{\partial\theta} - \frac{\partial\eta_k^3}{\partial\theta} = 0. \quad (33)\end{aligned}$$

Differentiating $\frac{\partial f_i}{\partial l_k}$ with respect to θ gives:

$$\frac{\partial^2 f_i}{\partial\theta\partial l_k} = \beta\left(\frac{\partial x_i}{\partial\theta}+\frac{\partial r_i}{\partial\theta}+\frac{\partial d_i}{\partial\theta}\right)T_1 - \beta\Big(1-x_i-r_i-d_i\Big)\Big[\delta_{ik}T_2+(1-\delta_{ik})T_3\Big], \quad (34)$$

where,

$$\begin{aligned}
T_1 &= \delta_{ik} \sum_{j \neq i} \mathcal{M}_{ij}(\theta - \theta^2 l_j)x_j + (1-\delta_{ik})(\theta - \theta^2 l_i)\mathcal{M}_{ik} x_k \\
T_2 &= \sum_{j \neq i} \mathcal{M}_{ij} \left[\left(1 - 2\theta l_j - \theta^2 \frac{\partial l_j}{\partial \theta} \right) x_j + (\theta - \theta^2 l_j) \frac{\partial x_j}{\partial \theta} \right] \\
T_3 &= \mathcal{M}_{ik} \left[\left(1 - 2\theta l_i - \theta^2 \frac{\partial l_i}{\partial \theta} \right) x_k + (\theta - \theta^2 l_i) \frac{\partial x_k}{\partial \theta} \right]
\end{aligned}$$

Substituting Eq. (34) into Eq. (33), we obtain an implicit equation including the derivative of the lockdown probability l_k with respect to θ, $\frac{\partial l_k}{\partial \theta}$, and other derivatives of lockdown probability l_j with respect to θ, $\frac{\partial l_j}{\partial \theta}$, for $j \neq k$. It follows that for all $k \in N^A$, we can not conclude whether $\frac{\partial l_k}{\partial \theta}$ is positive, negative or null. In fact, if we assume

$$\frac{\partial \mu_i^1}{\partial \theta} = \frac{\partial \eta_i^1}{\partial \theta} = \frac{\partial^2 f_i}{\partial \theta \partial l_k} = \frac{\partial \eta_k^2}{\partial \theta} = \frac{\partial \eta_k^3}{\partial \theta} = 0 \text{ for all } \forall i \in N \text{ and } k \in N^A,$$

then Eq. (33) becomes:

$$-(1-\alpha)p_k K^\alpha (1 - \theta l_k(\theta))^{-\alpha} - \alpha(1-\alpha)\theta p_k K^\alpha (l_k + \theta \frac{\partial l_k}{\partial \theta})(1 - \theta l_k)^{-\alpha - 1} + w_k = 0.$$

Then, we can express the derivative of lockdown with respect to lockdown effectiveness as

$$\frac{\partial l_k}{\partial \theta} = \frac{w_k - (1-\alpha)p_k K^\alpha (1 - \theta l_k)^{-\alpha-1}(1 - \theta l_k(1-\alpha))}{\alpha \theta^2 (1-\alpha) p_k K^\alpha (1 - \theta l_k)^{-\alpha - 1}}. \tag{35}$$

Since $(1-\alpha)p_k K^\alpha (1-\theta l_k)^{-\alpha-1}(1-\theta l_k(1-\alpha)) \geq 0$, then from Eq. (35), it is direct that the sign of $\frac{\partial l_k}{\partial \theta}$ can be either positive or negative depending on whether the wage w_k is greater or less than $(1-\alpha)p_k K^\alpha (1-\theta l_k)^{-\alpha-1}(1-\theta l_k(1-\alpha))$.

4 Simulations: FP vs NFP Nursing Homes and Lockdown Effectiveness

We present simulation results of the dynamic of epidemiological and economical outcomes for a social planner solving the problem (8) in Section 2. We choose the model parameters to match the period in which the U.S. nursing home networks was collected by the staff of the "Protect Nursing Homes" project.[10] After the national lockdown on nursing home visits introduced by the U.S. Federal government on March 13, 2020, the members of the "Protect Nursing Homes" project use geolocation data for 50 million smartphones during the 11-week study period to build the U.S. nursing home networks. They observe that 5.1% of smartphone users (approximately 501,503 staff and contractors) who visited a nursing home for at least 1 hour also visited another facility during the 11-week study period—even after visitor restrictions were imposed. In the nursing home network for each U.S. state, nodes denote individual nursing facilities. A connection is established between two nursing

[10]For more information on the Protect Nursing Homes project, we refer to the web-page https://protectnursinghmes.org and Chen et al. (2021).

homes, say I and II, if a staff of the nursing home I also visited the nursing home, II, for at least 1 hour. The intensity of connection between two nursing homes depends on the number of smartphones observed in both homes. Given the lack of accurate death data at the beginning of the COVID-19 pandemic, we use the data of the Centers for Medicare & Medicaid Services Data (CMS) from May 31 to August 16, 2020.[11]

Given the nature and complexity of our individual-based mean-field model for epidemic modeling on networks, we construct a representative network of nursing homes for Florida, as described in Figure 1, consisting of a sample of 85 nursing homes (58 FPs and 27 NFPs; Table 1 provides a brief descriptive statistics), ensuring the convergence of the system (ODE). Figure A1 in Appendix A provides the complete network of nursing homes in Florida.

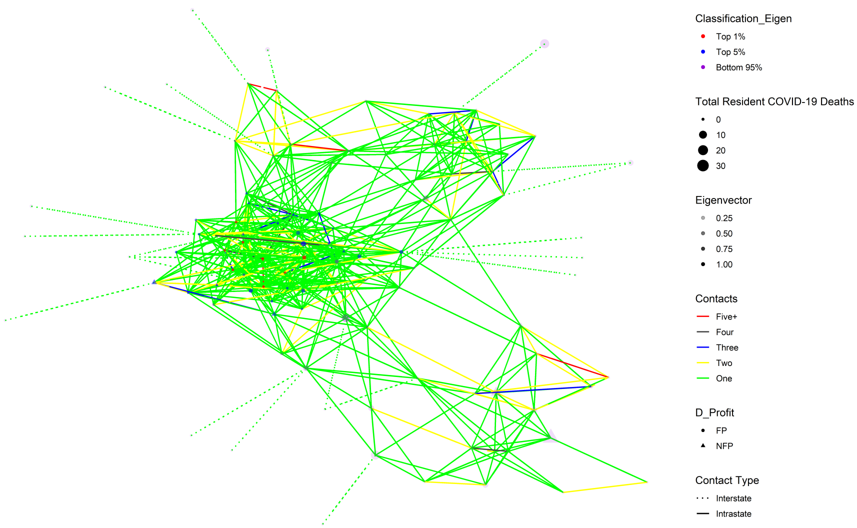

Fig. 1: Network structure for the 85 nursing homes in Florida, used in the simulations, with the eigenvector centrality measure. Notes: In the network, node size varies with the number of COVID-19 deaths among residents reported to the CMS as of May 31, 2020; shapes of nodes represent nursing homes' ownership, with the circle representing a FP nursing home, and a triangle representing a NFP nursing home; edge color differs with the number of contacts between nursing homes; a solid (resp. dotted) edge line corresponds to a connection between two nursing homes within the same U.S. state (resp. in two different states); and node color differences are based on eigenvector ranking, with the red color, for example, highlighting the top 1% of facilities with high eigenvector centrality in the network.

[11] COVID-19 nursing home data of the CMS are available at https://data.cms.gov/covid-19/covid-19-nursing-home-data.

Table 1: Descriptive statistics for the 85 nursing homes in Florida used in the simulations

Ownership	Number of nursing homes	COVID-19 deaths Min	Max	Mean	Sd	Eigenvector Min	Max	Mean	Sd
FP	58	0	18	1.19	3.09	0.0155	1	0.350	0.253
NFP	27	0	37	1.97	7.32	0.0339	0.702	0.329	0.246

Notes: Data are from the CMS as of May 31, 2020 and Chen et al. (2021). FP stands for a for-profit nursing home, NFP denotes a not-for-profit nursing home, and Sd means standard deviation.

To calibrate the epidemiological parameters β, κ, and γ, we use data from Statista[12] and Acemoglu et al. (2021). From Statista, the contact rate β is assumed to be 0.012. Following Acemoglu et al. (2021), we assume lifetime duration of the SARS-CoV-2 (the virus that causes COVID-19 disease) to be 18 days. Then, the recovery of an infected patient is governed by $\gamma = \frac{0.81}{18}$, and the death dynamics is driven by the parameter $\kappa = \frac{0.19}{18}$. In calibrating the production function, we consider $\chi_i^1 = 0$ and $\chi_i^2 = 1$, so that in Eq.(21), $h_i \approx (1-\theta l_i)$, and in Eq.(22), we have $y_i \approx k_i^{\alpha_i}(1-\theta l_i)^{1-\alpha_i}$, where y_i is the total number of residents (proxies the nursing home i's output) who receive care, k_i is the total number of beds (proxies the nursing home i's capital), and h_i is the number of occupied beds (proxies the nursing home i's labor supply). For illustration, we perform our simulations using nursing homes data for Florida. Summary statistics for the nursing homes in Florida with complete data are given in Table 2. As we show in Table 3, the estimated value of the elasticity of capital in Florida is $\alpha = 0.65$.

Table 2: Descriptive statistics of nursing homes in Florida

Variable	Mean (standard deviation)
COVID-19 death	O.82 (3.03)
Home eigenvector centrality	0.09 (0.15)
Regulatory measures	
For profit	0.7
Urban	0.95
Number of beds	120.17 (46.91)
Number of beds occupied	95.09 (41.22)
CMS quality rating (1-5)	4.02 (1.04)
Overall rating	3.46 (1.35)
County SES	343.55 (195.94)
Number of nursing homes	693

Notes: Data are from the CMS as of May 31, 2020 and Chen et al. (2021). Binary variables are percent of nursing homes; continuous variables are mean values, with standard deviations in parentheses.

[12]Statistica provides updated information on the reproduction number of COVID-19, and the rate of COVID-19 infection and death among nursing home residents in each U.S. state as of September 2020.

Table 3: Estimation of the nursing home production function in Florida

	(1)	(2)	(3)	(4)	(5)
log(h)	0.384***	0.364***	0.364***	0.364***	0.363***
	(15.36)	(15.17)	(15.17)	(15.17)	(15.16)
log(k)	0.647***	0.658***	0.658***	0.658***	0.658***
	(22.35)	(23.81)	(23.81)	(23.81)	(23.80)
County_ses	-0.000197	-0.000193	-0.000193	-0.000193	-0.000197
	(-0.95)	(-0.97)	(-0.97)	(-0.97)	(-0.99)
Overall_rating		0.0122**	0.0122**	0.0122**	0.0119**
		(2.11)	(2.11)	(2.11)	(2.05)
Dummy_urban				0.00457	0.00636
				(0.04)	(0.05)
D_Profit					0.00915
					(0.80)
Constant	-0.141*	-0.146*	-0.146*	-0.150	-0.161
	(-1.71)	(-1.82)	(-1.82)	(-1.08)	(-1.15)
County FE	YES	YES	YES	YES	YES
Observations	629	628	628	628	628
R^2	0.933	0.934	0.934	0.934	0.934

Notes: Data are from Chen et al. (2021). The dependent variable is the number of residents who receive care (y). Explanatory variables include the (log)-number of occupied beds ($\ln(h)$), the (log)-total number of beds ($\ln(k)$), the county's average socio-economic status (County_ses), the nursing home overall rating (Overall_rating), an indicator (Dummy_urban) for the nursing home location (1 if located in an urban area, and 0 otherwise), and an indicator (D_Profit) for the nursing home ownership status (1 if FP, and 0 otherwise), and county fixed effects (County FE). Standard errors are robust to heteroscedasticity of unknown form. t statistics in parentheses; p-values: $^{*}p < 0.1$, $^{**}p < 0.05$, $^{***}p < 0.01$.

Using data from the Bureau of Labor Statistics and the Senior Living project[13], the (average) price of the output is assumed to be the same for all the nursing homes $p_i = p = 38.58\$$ per hour and the (average) wage per hour is $w_i = w = 13.2\$$. In our simulations in Florida, we vary the tolerable infection incidence, ι, between 0.001, 0.005, and 0.01, and the parameter of lockdown effectiveness, θ, between 0.35, 0.5, and 0.9. We also complement simulation results in Florida with another set of dynamics in a random small-world network (Watts & Strogatz, 1998) with 1000 agents (700 FP and 300 NFP nursing homes), varying θ between 0.1, 0.5, and 0.9 with the calibrated parameters by Pongou et al. (2022b).

[13]We obtained information from the Senior Living project on September 9, 2021 at https://www.seniorliving.org/nursing-homes/costs/.

Simulation Results

We generate several optimal dynamics from the simulation results. For simplicity, we keep only the optimal lockdown and death dynamics in this section, and relegate the graphics that display the infection and surplus lost in Appendix A (Figs. A3 and A5, respectively).

Lockdown and surplus lost dynamics and lockdown effectiveness. We perform three sets of simulations for the optimal lockdown dynamics with three different values of ι and θ. The results are displayed in a two-dimensional graphic, with days on the horizontal axis, and the percentage of population sent into lockdown on the vertical axis. Fig. 2 displays the average optimal lockdown for FP and NFP nursing homes. In each period, a point in the graphic represents the average value of individual lockdown probabilities. In Fig. (2a) to Fig. (2f), we present three curves, each curve corresponding to a lockdown dynamics for a single value of ι, holding θ fixed. For any given level of lockdown effectiveness, the level of lockdown is larger in NFP nursing homes than in FP ones, whatever the tolerable infection incidence. As predicted in Proposition 2, the level of lockdown decreases with lockdown effectiveness for NFP nursing homes. The simulations concerning FP nursing homes in Florida seem to indicate that the average optimal lockdown increases with lockdown effectiveness. From Fig. 2, it holds that, if everything else is equal, when the effectiveness of lockdown increases, the number of NFP nursing homes that must be lockdown to achieve a normal profit decreases. The decrease in the number of NFP nursing homes in lockdown is compensated by an increase in the number of FP nursing homes in lockdown. It follows that the social planner trades locking down FP nursing homes for NFP ones as the lockdown effectiveness changes.[14] The results in Fig. A5 show that the economical cost (or surplus lost) of the lockdown is largely carried by NFP nursing homes in Florida. As hypothesised in the planner problem, NFP nursing homes suffer a total surplus lost, independently from the level of lockdown effectiveness. FP nursing homes seem to suffer a smaller surplus lost (less than 2% in all cases). Moreover, the economical lost in FP nursing homes increases with lockdown effectiveness.

As we point out in Remark 1, the lockdown dynamics in Florida do not ensure that we should expect a monotonic relationship between the optimal lockdown and lockdown effectiveness for FP nursing homes. For illustration purposes, we display in Fig. 3, the average optimal lockdown dynamics in a random small-world network, keeping the same values of ι, but varying θ between 0.1, 0.5, and 0.9. The simulation results in Fig. 3 show that, although the optimal lockdown is constant in FP nursing homes, it is not monotonic in

[14] For robustness, we also illustrate how lattice, random, scale-free, and small-world network structures affect optimal lockdown rates, disease, and economic dynamics in FP and NFP nursing homes, respectively. As in Florida, we note that the average lockdown probability increases with lockdown effectiveness in FP nursing homes in each network structure. In contrast, it decreases with lockdown effectiveness in NFP nursing homes. Since the network structures are different, for each profile (θ, ι), the lockdown policies translate to different infection and surplus lost dynamics for each network. For simplicity, we omit the figures showing these dynamics in the paper. All figures can be obtained upon request.

FP nursing homes. It increases from when moving from $\theta = 0.1$ to $\theta = 0.5$, but decreases from $\theta = 0.5$ to $\theta = 0.9$.

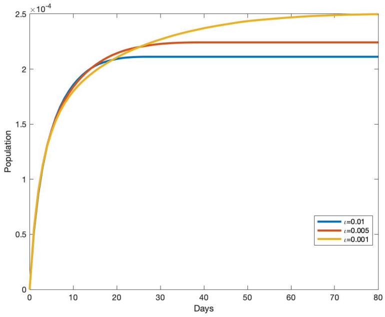

(a) Lockdown in FPs with $\theta = 0.9$

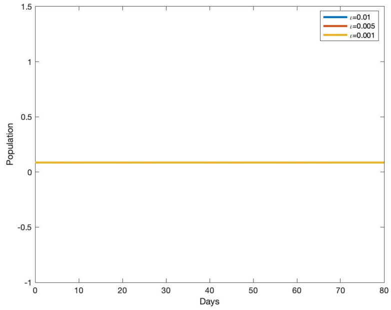

(b) Lockdown in NFPs with $\theta = 0.9$

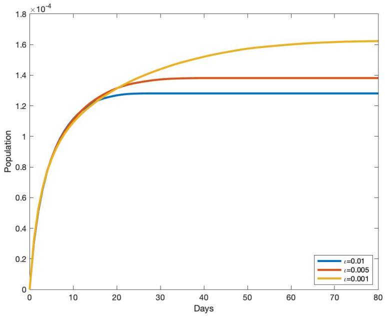

(c) Lockdown in FPs with $\theta = 0.5$

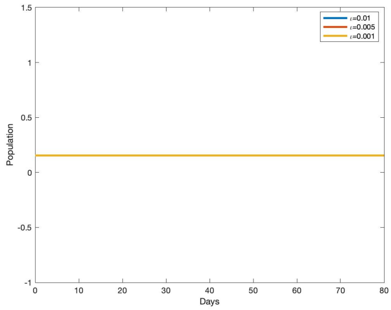

(d) Lockdown in NFPs with $\theta = 0.5$

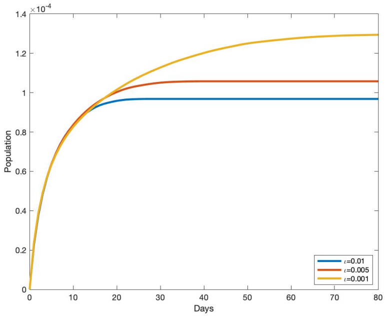

(e) Lockdown in FPs with $\theta = 0.35$

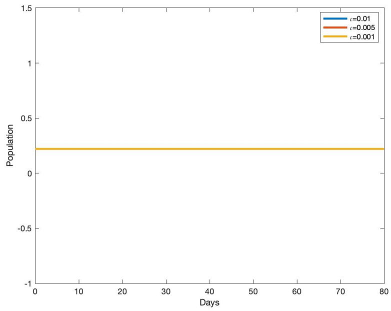

(f) Lockdown in NFPs with $\theta = 0.35$

Fig. 2: Optimal lockdown and lockdown effectiveness in Florida.

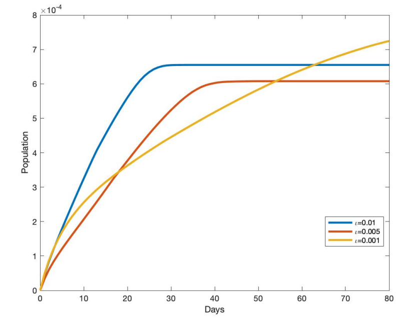

(a) Lockdown in FPs with $\theta = 0.9$

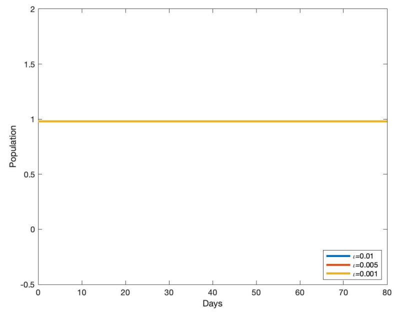

(b) Lockdown in NFPs with $\theta = 0.9$

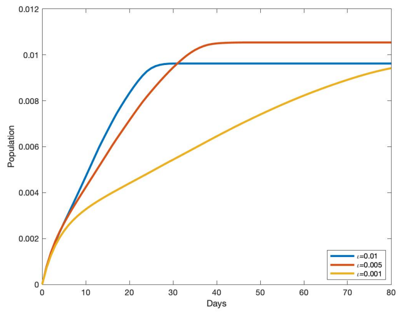

(c) Lockdown in FPs with $\theta = 0.5$

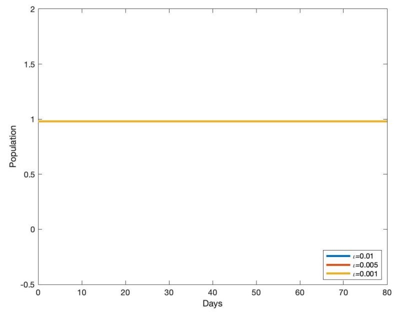

(d) Lockdown in NFPs with $\theta = 0.5$

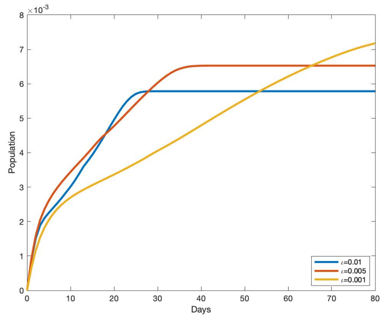

(e) Lockdown in FPs with $\theta = 0.1$

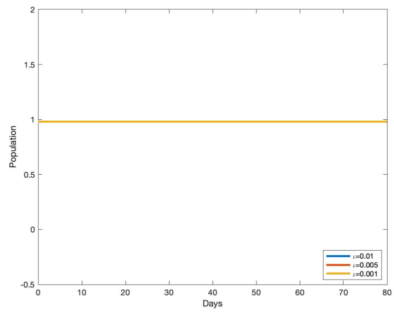

(f) Lockdown in NFPs with $\theta = 0.1$

Fig. 3: Optimal lockdown and lockdown effectiveness in a random small-world network.

Infection and death dynamics. Fixing θ, we perform three sets of simulations with three different values of ι. The results are displayed in a two-dimensional graphic, with days on the horizontal axis, and the percentage of population affected for the variable (infection or death) on the vertical axis. In each period, a point in the graphic represents the average value of individual probabilities. For the surplus lost, the vertical axis represents the percentage of economic surplus lost relative to the economy without the pandemic. Each graph shows three dynamics for a single variable of interest and a given value of ι. The graphics in Fig. A3 show that, independently of lockdown effectiveness, a higher tolerable infection incidence (ι) leads to an increase of infections at the initial stages of the pandemic. However, FP nursing homes experience a slightly more infections than NFP nursing homes. In the long-run all the infection dynamics are virtually similar in FP and NFP nursing homes whatever the values of θ and ι. As we show in Fig. 4, these infection dynamics translate to similar death dynamics for higher values of ι in FP and NFP nursing homes. Also, in Fig. 4, the death differential between FP and NFP nursing homes in Florida as function of the lockdown effectiveness is insignificant. However, the simulation results in the random small-world network (see Figs. A4, 5, and A6 for infection, deaths, and surplus lost, respectively) overturn the latter observation. We note that the difference in death dynamics between FP and NFP nursing homes in Fig. 5 becomes more apparent when lockdown effectiveness is large. Our simulation outcomes suggest that, in addition to the ownership status of nursing homes, the lockdown effectiveness can contribute to the factors explaining the death differential observed between FP and NFP nursing homes in the United States. Our empirical application in Section 5 offers a complementary discussion on this issue.

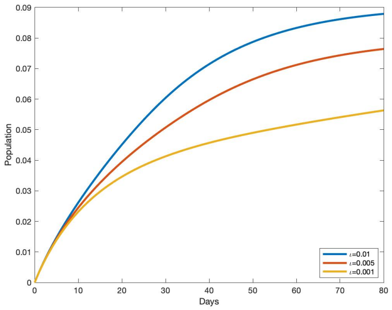

(a) Deaths in FPs with $\theta = 0.9$

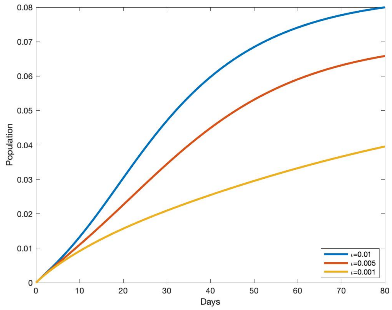

(b) Deaths in NFPs with $\theta = 0.9$

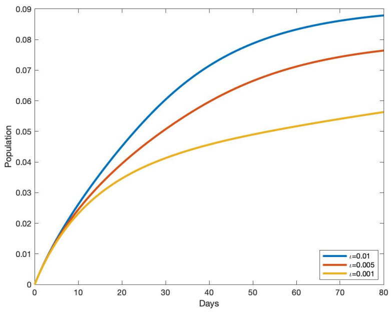

(c) Deaths in FPs with $\theta = 0.5$

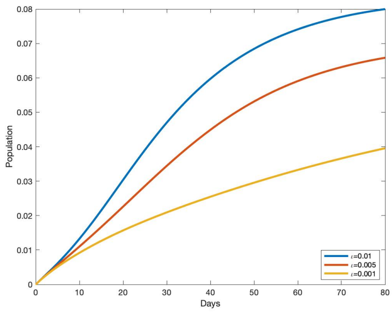

(d) Deaths in NFPs with $\theta = 0.5$

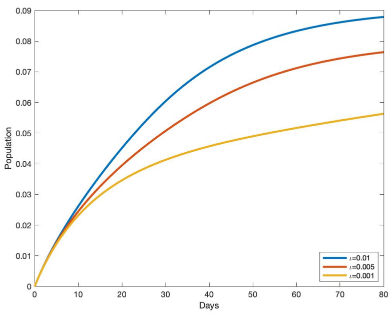

(e) Deaths in FPs with $\theta = 0.35$

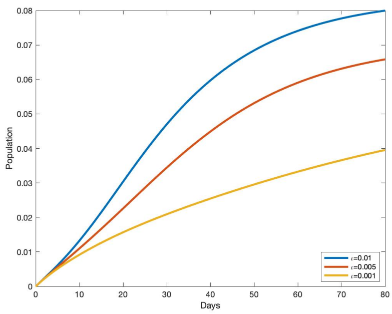

(f) Deaths in NFPs with $\theta = 0.35$

Fig. 4: Deaths dynamics and lockdown effectiveness in Florida.

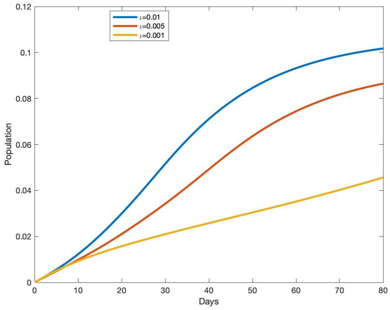

(a) Deaths in FPs with $\theta = 0.9$

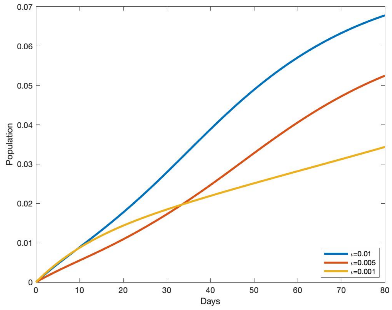

(b) Deaths in NFPs with $\theta = 0.9$

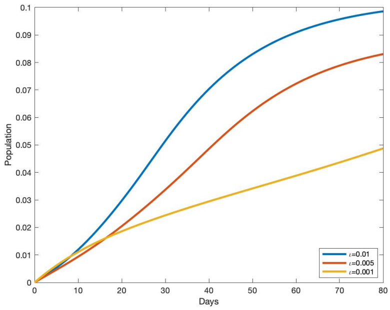

(c) Deaths in FPs with $\theta = 0.5$

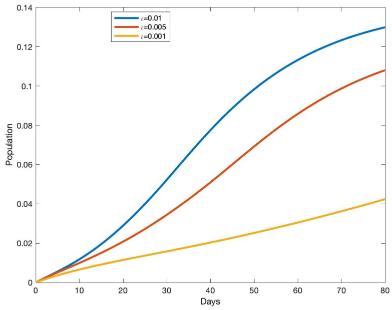

(d) Deaths in NFPs with $\theta = 0.5$

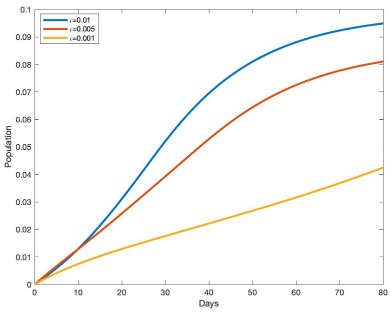

(e) Deaths in FPs with $\theta = 0.1$

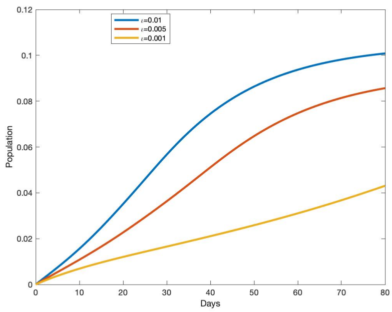

(f) Deaths in NFPs with $\theta = 0.1$

Fig. 5: Deaths dynamics and lockdown effectiveness in a random small-world network.

5 Empirical Application

In this section, we use data on U.S nursing homes to estimate the level of lockdown effectiveness (θ) and the tolerated COVID-19 infection incidence (ι) in U.S. states. Using the estimated values, we test the hypotheses H_1 and H_2 stated in Section 4.

5.1 Data, Calibration, and Estimation of $\boldsymbol{\theta}$ and $\boldsymbol{\iota}$

We calibrate the two-sector N-SIRD model introduced in Section 2 using data on nursing homes from several sources. We collect the data to reflect the reality of nursing homes during our study period, between May 31 and August 16, 2020. Data on the economic variables come from the Bureau of Labor Statistics and the Senior Living project. We use samples of nursing home networks collected by Chen et al. (2021) and the project "Protect Nursing Homes" hosted at Yale University. For clarity, we summarize in Table B1 in Appendix B all relevant sources of data that we use to calibrate the epidemiological and economic parameters of interest.

We use a simulated minimum distance estimator to estimate the lockdown effectiveness (θ) and the tolerated incidence (ι) for 40 U.S. states. In each nursing home network, a node is represented by a nursing home. The nursing home ownership (FP or NFP) is assigned from the data. The connection between two nursing homes is established if the same smartphone signal is recorded in the locations of these two care homes. The number of distinct signals gives the weight of the connection (or link) between two nursing homes. The simulation process derives the values of θ and ι that minimizes the distance between the simulated COVID-19 death dynamic of the calibrated model and the raw data from the CMS from May 31 to August 16, 2020 in the nursing homes of the 40 U.S. states.

Formally, let us index a U.S. state by $s \in \overline{S}$, with $\overline{S} = \{1, ..., 40\}$. Let d_{ts} denote the number of COVID-19 deaths observed at time $t = 1, ..., T$ in the U.S. state $s \in \overline{S}$. For each value of the parameter profile (ι, θ), where ι is the tolerable infection incidence, and θ is the lockdown effectiveness, we can simulate death dynamics denoted as $\hat{d}_{ts}(\iota, \theta)$. Since our simulations are deterministic, there is no random shock in our model. Thus, repeating the simulations with the same initial conditions produce the same outcomes. For each U.S. state $s \in \overline{S}$, we estimate the parameter profile (ι, θ) that we denote as $(\hat{\iota}_s, \hat{\theta}_s)$ by solving the following minimization problem:

$$(\hat{\iota}_s, \hat{\theta}_s) = argmin \left\{ \sum_{t=1}^{T} (\hat{d}_{ts}(\iota, \theta) - d_{ts})^2 \right\}, \ (\iota, \theta) \in [0, 1]^2. \tag{36}$$

Existing literature on simulated minimum distance estimators (e.g., Gertler and Waldman (1992), and Forneron and Ng (2018)) suggests that $(\hat{\iota}_s, \hat{\theta}_s)$ is a consistent estimator of the parameter profile (ι_s, θ_s) for the U.S. state $s \in \overline{S}$. From the estimated values of lockdown effectiveness that we provide in Figure

6, the average lockdown effectiveness is 0.53 with a standard deviation of 0.38, and the median is, $\theta_m = 0.665$. The minimum lockdown effectiveness is 2.93×10^{-11}, in South Dakota, and the maximum lockdown effectiveness is achieved in New York at 0.973. For simplicity, we plot the estimated values of the tolerated COVID-19 infection incidence in Figure A2 in Appendix A. The average COVID-19 tolerable infection incidence is 0.33 with a standard deviation of 0.22. The tolerance infection incidence is minimal in Connecticut (2.09×10^{-9}) and maximal in New Hampshire (0.657). In Section 5.2, we provide some factors that may explain the heterogeneity of the estimated values of $\hat{\theta}_s$.

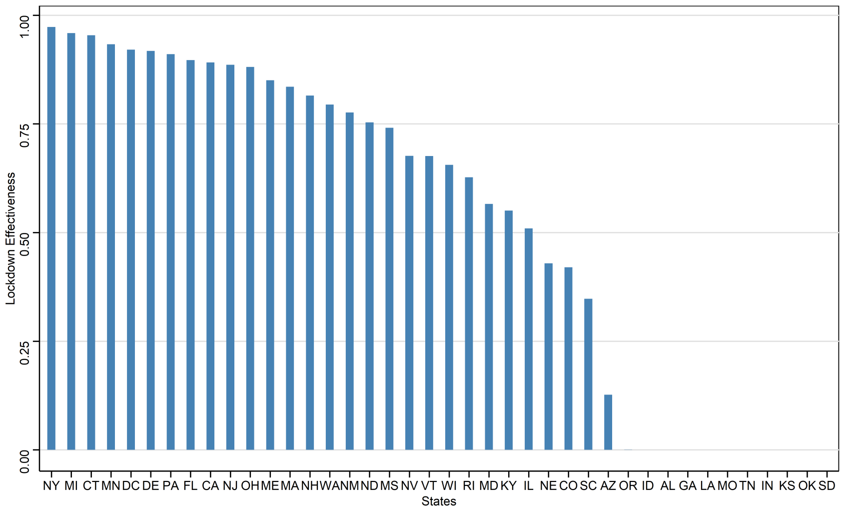

Fig. 6: Lockdown effectiveness across U.S. state (θ). Notes: The parameter θ estimates the lockdown effectiveness of the U.S. state governor from May 31 to August 16, 2020. Using the CMS data and the calibrated parameters in the model, we estimate θ for 40 U.S. states. The average value of estimates is 0.53 and the standard deviation is 0.38.

In line with other studies tracking planners' actions towards mitigating the pandemic (Hale et al., 2021), we perform a simple investigation on the relationship between our approach to capturing tolerable infection incidence and lockdown effectiveness with other indicators designed by the members of the Oxford COVID-19 Government Response Tracker (OxCGRT) from May 31 to August 16, 2020. Tracking national and, for some countries (e.g., U.S), subnational governments' policies and interventions across a standardized series of indicators, the OxCGRT's project created a suite of composite indexes, including the stringency index (SI), the containment and health index (CHI), the more comprehensive government response index (GRI) and the economic support index (ESI). The index SI exclusively assesses the extent of closure and containment policies. In addition to the indicators that define SI, the index CHI also includes health system policies such as public information campaign, testing, and contract tracing policies. ESI provides a holistic measure of financial assistance to households, and GRI is an overall measure of the government's policies (pharmaceutical and non-pharmaceutical) during the COVID-19 pandemic. Along with other key variables that we use in the study, we summarize in Table 4 the descriptive statistics of the OxCGRT indices.

Table 4: Descriptive statistics of U.S. nursing homes and U.S. states data

Nursing Homes	
Variable	Mean (standard deviation)
Regulatory measures	
For profit	0.69
Urban	0.74
Number of beds	107.09 (61.65)
Number of beds occupied	78.72 (50.72)
CMS quality rating (1-5)	3.76 (1.23)
Overall rating	3.23 (1.42)
COVID-19 death	2.16 (6.47)
Home eigenvector centrality	0.09 (0.19)
Number of nursing homes	12366
U.S. states (40 states)	
Variable	Mean (standard deviation)
Republican Governor	0.48
Female Governor	0.2
South	0.28
Governor Approval	56.11 (9.3)
GDP Growth	-3.51 (1.36)
County SES	404.42 (276.84)
Tolerable infection incidence	0.33 (0.22)
Lockdown effectiveness	0.53 (0.38)
Stringency Index	63.25 (8.80)
Government Response Index	61.87 (7.66)
Containment Health Index	60.92 (7.41)
Economic Support Index	68.55 (14.42)

Notes: Data are from the CMS as of May 31, 2020, Chen et al. (2021), Hale et al. (2021), and the COVID STATES PROJECT. Binary variables are percent of nursing homes; continuous variables are mean values, with standard deviations in parentheses.

Focusing on the U.S., we provide in Table 5 a simple correlation between θ, ι, and the OxCGRT indexes. Our results in Table 5 show that the lockdown effectiveness is positively and significantly correlated with all the OxCGRT indexes. Additionally, while ι is positively correlated with SI and ESI, it is negatively correlated with GRI and CHI, and all these correlations are not significant. We should note that removing θ as controls in Table 5 overturns the not-significance of ι with all the OxCGRT indexes. The latter shows that the lockdown effectiveness captures all the explanatory power of ι in explaining government responses during the pandemic. From Table 5, we note that higher lockdown effectiveness during the pandemic results from government financial support and stringent containment policies.

Table 5: Correlation between θ, ι, and OxCGRT indexes

	Stringency Index	Government Response Index	Containment Health Index	Economic Support Index
θ	12.11***	11.09***	10.70***	13.85***
	(23.52)	(26.06)	(25.97)	(11.97)
ι	0.933	-0.115	-0.569	3.083
	(1.05)	(-0.16)	(-0.80)	(1.54)
Constant	56.50***	56.01***	55.42***	60.16***
	(190.78)	(228.78)	(233.87)	(90.37)
Observations	3120	3120	3120	3120
R^2	0.229	0.256	0.249	0.079

Notes: Data are from Hale et al. (2021) and authors' estimations. t statistics in parentheses. * $p < 0.1$, ** $p < 0.05$, *** $p < 0.01$.

5.2 Explaining Heterogeneity of Lockdown Effectiveness (θ) across U.S. States

To investigate the sources of heterogeneity in the lockdown effectiveness across the 40 U.S. states, we perform a simple OLS regression using the estimated values of $\hat{\theta}_s$ and $\hat{\iota}_s$ and some U.S. states' characteristics. The results in Table 6 show that institutional and political factors, nursing homes' ownership, the pandemic severity and government responses, and geographical locations play a significant role in the determination of the levels of θ.[15]

Using the estimations in Columns (1) to (Main) in Table 6, we note that the lockdown effectiveness is lower in U.S. states with Republican governors. Governors with higher level of approval in opinions pools tend to have more effective lockdown in their states. States with more FP nursing homes experience lower lockdown effectiveness, with republican run states having slightly higher levels. In Column (4), U.S. states with high lockdown effectiveness experience higher COVID-19 death count. This correlation is a result of imposing more stringent policies as response of more pandemic fatalities in the state.

[15] One can perform a similar analysis in explaining the variation of ι across U.S. states. Pongou et al. (2022b) provide such analysis for an N-SIRD model with lockdown when the lockdown effectiveness is $\theta = 1$ and there is only one type of nursing homes.

Moreover, from Column (6), interacting the state governor's political affiliation with COVID-19 death count, we note that the effects of COVID-19 death on lockdown effectiveness is more pronounced in Republican states. The latter implies that, an increase in the state COVID-19 death count decreases the gap in lockdown effectiveness between Democrat and Republican-run states. In Column (7), states located in the South experience lower lockdown effectiveness. However, the interaction terms Republican$\times$South yield positive and significant effects on θ.

We also note in Table 6 that U.S. states with higher GDP growth have lower lockdown effectiveness, as shown in Columns (9) and (Main). Indeed, during the study period, all states experience negative GDP growth. A significant decline in GDP worldwide resulted from lockdown and containment policies enforced by governments and policymakers to mitigate the COVID-19 pandemic. Thus, higher growth can be associated with less strict policies (higher ι).[16] The relationship between economic prosperity and the effectiveness of lockdown is stronger in republican-led states. Table 6 also suggests a positive association between θ and ι. We discuss the impact of such a relationship in the COVID-19 deaths in Section 5.3. Column (4) shows that the lockdown effectiveness increases as the number of COVID-19 deaths increases. A rationale for this result is that a higher number of COVID-19 deaths increases the population's awareness and compliance with recommendations of public health authorities, which thus leads to higher lockdown effectiveness. However, the effect of COVID-19 deaths on lockdown effectiveness differs between FP and NFP nursing homes (Columns (5) to (Main)). In fact, a reduction in the number of COVID-19 deaths is predicted to increase the lockdown effectiveness in states with more NFP nursing homes but decrease the lockdown effectiveness in states with more FP nursing homes in republican-run states.

Overall, all the findings are robust when we also control for the OxCGRT indices (SI, CHI, and GRI). For clarity, we report the robustness checks in Table B2 in Appendix B. The results are in line with the relationship between the lockdown effectiveness and the government pandemic responses that we highlight in Table 5.

[16] Although our analysis uses U.S. data, we can offer similar conjectures in developing countries like those in Sub-Saharan Africa (SSA). As we mentioned in the Introduction, enforcing an effective lockdown strategy in a pandemic like COVID-19 in SSA requires significant government financial support since more than 80% of people in the workforce find their livelihoods in the informal sector (Nguimkeu, 2014; Nguimkeu & Okou, 2021). This might explain why several African countries have relied on less costly mitigating strategies such as mask-wearing and hand washing while waiting for the arrival of COVID-19 vaccines.

Table 6: Explaining lockdown effectiveness heterogeneity in U.S. states

	(1)	(2)	(3)	(4)	(5)	(6)	(7)	(8)	(9)	(Main)
ι	0.834***	0.844***	0.847***	0.839***	0.840***	0.840***	0.827***	0.834***	0.837***	0.828***
	(48.01)	(48.80)	(49.21)	(47.20)	(47.35)	(47.33)	(45.65)	(49.04)	(49.93)	(48.74)
Republican	-0.100***	-0.100***	-0.184***	-0.186***	-0.190***	-0.191***	-0.179***	-0.238***	-0.228***	-0.275***
	(-16.10)	(-16.09)	(-18.86)	(-18.54)	(-18.70)	(-18.76)	(-17.42)	(-23.68)	(-22.75)	(-16.87)
Governor Approval	0.00986***	0.00981***	0.00989***	0.00987***	0.00986***	0.00984***	0.00897***	0.0112***	0.0103***	0.0102***
	(31.28)	(31.08)	(31.45)	(30.24)	(30.21)	(30.12)	(27.98)	(35.30)	(34.06)	(34.34)
Economic Support Index	0.00399***	0.00398***	0.00418***	0.00415***	0.00416***	0.00416***	0.00443***	0.00332***	0.00342***	0.00365***
	(20.64)	(20.47)	(21.77)	(20.77)	(20.79)	(20.80)	(22.05)	(17.04)	(17.73)	(17.72)
D_Profit		-0.0421***	-0.0982***	-0.0986***	-0.107***	-0.107***	-0.103***	-0.0916***	-0.0853***	-0.0873***
		(-7.85)	(-13.22)	(-12.86)	(-13.12)	(-13.08)	(-12.77)	(-11.72)	(-10.87)	(-11.08)
Republican× D_Profit			0.125***	0.126***	0.131***	0.130***	0.133***	0.105***	0.0939***	0.0949***
			(11.76)	(11.40)	(11.67)	(11.61)	(11.86)	(9.63)	(8.58)	(8.67)
Covid_Death				0.000713**	-0.00168***	-0.00190***	-0.00182***	-0.00221***	-0.00258***	-0.00244***
				(2.35)	(-2.71)	(-3.13)	(-3.08)	(-3.71)	(-4.34)	(-4.14)
Covid_Death×D_Profit					0.00325***	0.00319***	0.00307***	0.00288***	0.00273***	0.00277***
					(4.61)	(4.51)	(4.43)	(4.11)	(3.91)	(4.02)
Republican×Covid_Death						0.00132*	0.00140*	0.00186**	0.00238***	0.00213***
						(1.66)	(1.75)	(2.31)	(3.07)	(2.76)
South							-0.0592***	-0.247***	-0.255***	-0.251***
							(-9.03)	(-26.96)	(-26.74)	(-26.52)
Republican×South								0.322***	0.319***	0.312***
								(26.01)	(25.40)	(24.48)
GDP_Growth									-0.0204***	-0.0143***
									(-11.39)	(-5.78)
Republican×GDP_Growth										-0.0138***
										(-3.52)
Constant	-0.485***	-0.456***	-0.438***	-0.431***	-0.426***	-0.424***	-0.385***	-0.419***	-0.452***	-0.437***
	(-24.24)	(-22.01)	(-20.92)	(-19.81)	(-19.48)	(-19.37)	(-17.43)	(-19.37)	(-21.51)	(-20.84)
Observations	12348	12348	12348	11535	11535	11535	11535	11535	11535	11535
R^2	0.521	0.524	0.529	0.527	0.528	0.528	0.531	0.555	0.558	0.558

Notes: Data are from the CMS as of May 31, 2020, Chen et al. (2021), Hale et al. (2021), the COVID STATES PROJECT, and authors' estimations. The dependent variable is the estimated value of θ at the U.S. state. We provide in Table B2 some robustness checks of Table 6 with other OxCGRT indexes. t statistics in parentheses. $^{*}p < 0.1$, $^{**}p < 0.05$, $^{***}p < 0.01$.

5.3 Lockdown Effectiveness and Death in Nursing Homes

In Section 2, we interact epidemiology and economics to contribute to the ongoing literature that explores the origin of the COVID-19 death gap observed between FP and NFP nursing homes; for a brief survey, see, e.g., Bach-Mortensen et al. (2021). Our simulation results suggest that the lockdown effectiveness could be a critical factor in explaining the associations between care home ownership and COVID-19 mortality in U.S. nursing homes. We estimate the effects of the lockdown effectiveness on the COVID-19 deaths in nursing homes and how this effect varies between pandemic mitigation policies and the ownership of nursing homes using the following equation:

$$\begin{aligned}\text{covid\_death}_{ijs} &= d_0\theta_s + a_1\text{Eig\_Cent}_{ijs} + a_2\text{County\_ses}_{js} \\ &+ a_3\text{D\_Profit}_{ijs} + d_1\theta_s \times \text{Eig\_Cent}_{ijs} \\ &+ d_2\theta_s \times \text{County\_ses}_{js} + d_3\theta_s \times \text{D\_Profit}_{ijs} \\ &+ c'X_{ijs} + \delta_j + \varepsilon_{ijs},\end{aligned} \tag{37}$$

where covid_death_{ijs} is a variable counting the total number of COVID-19 deaths in the nursing home i located in county j and state s; θ_s is the lockdown effectiveness level in U.S. state s; Eig_Cent_{ijs} is the eigenvector centrality index for the nursing home i; County_ses_{js} is the county j's average socio-economic status; D_Profit_{ijs} is an indicator for whether nursing home i is FP (1 if FP, and 0 if NFP); X_{ijs} represents other exogenous characteristics of the nursing home including the constant; and δ_j is the county fixed effect. We report our main results in Table 7.

Table 7: Estimating the effects of lockdown effectiveness on COVID-19 deaths in U.S. nursing homes

	(1)	(2)	(3)	(4)	(Main_Death)
θ	0.622***	0.623***	0.633***	0.656***	0.654***
	(3.36)	(3.37)	(3.41)	(3.52)	(3.51)
D_Profit	0.154	0.170	0.183	-0.678***	-0.668***
	(1.18)	(1.30)	(1.39)	(-4.33)	(-4.09)
Eig_Cent	3.785***	1.717***	3.791***	3.766***	2.663***
	(8.34)	(2.77)	(8.36)	(8.32)	(4.18)
Overall Rating	-0.167***	-0.166***	-0.168***	-0.168***	-0.168***
	(-3.81)	(-3.79)	(-3.83)	(-3.85)	(-3.83)
Governor Approval	0.0871***	0.0826***	0.0811***	0.0770***	0.0760***
	(11.72)	(11.09)	(10.91)	(10.42)	(10.23)
Stringency Index	0.0135	0.0180**	0.0222***	0.0288***	0.0292***
	(1.62)	(2.17)	(2.64)	(3.41)	(3.45)
County_ses	0.00854***	0.00828***	0.00726***	0.00777***	0.00792***
	(7.42)	(7.23)	(6.02)	(6.78)	(6.66)
$\theta\times$ Eig_Cent		4.477***			2.384*
		(3.74)			(1.94)
$\theta\times$ County_ses			0.00185***		-0.000403
			(4.36)		(-0.98)
$\theta\times$ D_Profit				1.937***	1.919***
				(6.96)	(6.49)
Constant	-3.456***	-3.516***	-3.709***	-3.965***	-3.937***
	(-4.37)	(-4.45)	(-4.66)	(-4.97)	(-4.94)
County FE	Yes	Yes	Yes	Yes	Yes
Observations	11406	11406	11406	11406	11406
R^2	0.085	0.086	0.086	0.088	0.088

Notes: Data are from the CMS as of May 31, 2020, Chen et al. (2021), Hale et al. (2021), and authors' estimations. The dependent variable is the number of COVID-19 deaths in a nursing home. We provide in Table B3 some robustness checks of Table 7 with other OxCGRT indexes. t statistics in parentheses. $^{*}p < 0.1$, $^{**}p < 0.05$, $^{***}p < 0.01$.

In Column (1), we control for θ, the nursing home ownership, the eigenvector centrality of a nursing home, the quality rating, the governor approval, the stringency index, and the county socio-economic status. Increasing θ by five standard deviations raises on average the number of deaths in a nursing home by approximately 1.18. In Table 6, we note a positive and significant correlation between the governor's tolerance toward the virus and the state's lockdown effectiveness. In other words, governors in U.S. states with higher lockdown effectiveness are inclined to enforce less stringent lockdown strategies to mitigate the pandemic. The planner may achieve their objectives by setting effective targeting lockdown policies that only confine a small fraction of the population (e.g., the group containing the patient zero) and allow others to keep the economy afloat. Although this planning decision may work in the short-run, the findings in Column (1) suggest that the long-run effects of such planning decisions can be detrimental to population health as the infection leads to a significant burden of deaths. Therefore, the governor should reverse their mitigation strategies and enforce more rigid pandemic responses in these situations. In Column (1), we also note that U.S. states with a high proportion of FP nursing homes experience more deaths (although not statistically significant at 10% level); a ten-percentage point increase in the proportion of FP nursing homes is associated with an expected increase in the number of deaths by over 1.5.

In Table 7, nursing homes that occupy more central positions (i.e., nursing homes with high eigenvector centrality) in networks endure a large COVID-19 mortality. In Column (2), we interact the level of centrality with the measure of lockdown effectiveness and find that the death count gap between more central nursing homes increases with lockdown effectiveness. In Column (3), we control for the interaction term between County_ses and θ, finding a positive effect. Thus, as the lockdown becomes more effective, nursing homes located in richer counties are expected to experience more COVID-19 death than nursing homes located in poorer counties. In contrast to Columns (1) to (3), the effects of the lockdown effectiveness on Covid-death in Column (4) and (Main_Death) are also mediated by nursing home ownership. In Column (4), controlling for the interaction term between D_Profit and θ, we find a positive effect. We obtain a similar result in Column (Main_Death) where we control for all variables. These findings suggest that the excess death in FP nursing homes relative to NFP homes is larger in U.S. states with a high lockdown effectiveness. This result aligns with the simulation results stating that higher lockdown effectiveness exacerbates the death differential between FP and NFP nursing homes. Therefore, lockdown effectiveness plays a crucial role in explaining the FP-vs-NFP COVID-19 death gap documented in the literature (Bach-Mortensen et al., 2021). Our results are robust when controlling for other additional factors; see Table B3 in Appendix B.

Pushing the analysis a little bit further, we provide two other regression results. We consider a lockdown policy to be highly effective if the lockdown effectiveness, θ, is greater than its median value θ_m, and the lockdown strategy to be partial or less effective if θ is less or equal than θ_m. Table 8 reports the results in U.S. states with less effective lockdown strategies ($\theta \leq \theta_m$) and Table 9 reports the results in U.S. states with less effective lockdown strategies ($\theta > \theta_m$). These analyses follow the simulation results (Figs. 4 and 5) showing that the lockdown effectiveness is a factor to consider in explaining the COVID-19 death gap between FP and NFP nursing homes. Indeed, the for-profit status of the nursing home only affects the number of COVID-19 death in U.S. states with highly effective lockdown strategies; see Columns (1) to (3) in Table 9.

Table 8: Estimating the effects of lockdown effectiveness on the number of COVID-19 deaths in nursing homes in U.S. states with less effective lockdown strategies

	(1)	(2)	(3)	(4)	(5)
θ	-0.204	-0.195	-0.245	-0.220	-0.235
	(-0.97)	(-0.93)	(-1.15)	(-1.05)	(-1.09)
D_Profit	0.0252	0.0276	0.0258	0.204	0.226
	(0.22)	(0.25)	(0.23)	(1.03)	(1.05)
Eig_Cent	1.987***	1.611**	1.976***	1.965***	1.254*
	(5.37)	(2.46)	(5.32)	(5.30)	(1.77)
Overall Rating	-0.180***	-0.179***	-0.180***	-0.180***	-0.179***
	(-4.73)	(-4.72)	(-4.74)	(-4.73)	(-4.71)
Governor Approval	0.0565***	0.0550***	0.0608***	0.0604***	0.0610***
	(5.71)	(5.42)	(5.25)	(5.76)	(5.25)
Stringency Index	0.0211***	0.0220***	0.0182**	0.0186**	0.0181**
	(2.67)	(2.79)	(2.14)	(2.33)	(2.13)
County_ses	0.0000952	0.0000621	0.000447	0.000180	0.000369
	(0.11)	(0.07)	(0.46)	(0.20)	(0.38)
$\theta\times$ Eig_Cent		0.853			1.595
		(0.56)			(0.98)
$\theta\times$ County_ses			-0.000493		-0.000341
			(-0.96)		(-0.64)
$\theta\times$ D_Profit				-0.383	-0.419
				(-1.09)	(-1.00)
Constant	-2.684***	-2.666***	-2.738***	-2.741***	-2.750***
	(-3.91)	(-3.87)	(-3.93)	(-3.95)	(-3.93)
County FE	Yes	Yes	Yes	Yes	Yes
Observations	5169	5169	5169	5169	5169
R^2	0.128	0.128	0.128	0.128	0.128

Notes: Data are from the CMS as of May 31, 2020, Chen et al. (2021), Hale et al. (2021), and authors' estimations. The dependent variable is the number of COVID-19 deaths in a nursing home. We provide in Table B4 some robustness checks of Table 8 with other OxCGRT indexes. t statistics in parentheses. $^{*}p < 0.1$, $^{**}p < 0.05$, $^{***}p < 0.01$.

Table 9: Estimating the effects of lockdown effectiveness on COVID-19 deaths in nursing homes in U.S. states with highly effective lockdown strategies

	(1)	(2)	(3)	(4)	(5)
θ	9.811***	9.219***	8.486***	7.639***	7.804***
	(5.05)	(4.76)	(4.21)	(3.92)	(3.88)
D_Profit	0.383*	0.389*	0.413*	-0.617***	-0.699***
	(1.72)	(1.74)	(1.83)	(-2.64)	(-2.84)
Eig_Cent	4.833***	2.284**	4.799***	4.686***	2.968***
	(6.03)	(2.04)	(5.98)	(5.86)	(2.68)
Overall Rating	-0.165**	-0.164**	-0.168**	-0.169**	-0.167**
	(-2.27)	(-2.26)	(-2.32)	(-2.33)	(-2.30)
Governor Approval	0.0984***	0.0956***	0.0980***	0.0949***	0.0930***
	(8.28)	(8.11)	(8.27)	(8.11)	(7.96)
Stringency Index	-0.0252	-0.0174	-0.0103	0.0113	0.0110
	(-1.46)	(-1.02)	(-0.59)	(0.63)	(0.62)
County_ses	0.0145***	0.0143***	0.0134***	0.0133***	0.0137***
	(6.72)	(6.61)	(6.04)	(6.20)	(6.34)
$\theta\times$ Eig_Cent		5.283***			3.576*
		(2.76)			(1.91)
$\theta\times$ County_ses			0.00194***		-0.00105
			(2.90)		(-1.58)
$\theta\times$ D_Profit				2.363***	2.530***
				(5.92)	(5.94)
Constant	-9.489***	-9.353***	-9.336***	-9.955***	-9.979***
	(-3.74)	(-3.69)	(-3.68)	(-3.94)	(-3.93)
County FE	Yes	Yes	Yes	Yes	Yes
Observations	6237	6237	6237	6237	6237
R^2	0.090	0.091	0.091	0.094	0.094

Notes: Data are from the CMS as of May 31, 2020, Chen et al. (2021), Hale et al. (2021), and authors' estimations. The dependent variable is the number of COVID-19 deaths in a nursing home. We provide in Table B5 some robustness checks of Table 9 with other OxCGRT indexes. t statistics in parentheses. $^{*}p < 0.1$, $^{**}p < 0.05$, $^{***}p < 0.01$.

6 Conclusion

This study addresses the problem of finding an optimal non-pharmaceutical intervention to mitigate the spread of a contagion in an undirected network of physical contacts, and it shows how such an intervention affects for-profit and not-for-profit organizations differently. The planner's tolerable infection incidence—preference for enforcing a stringent containment strategy—depends on its effectiveness, i.e., how the chosen intervention can effectively reduce the contagion. Using lockdown as a control variable, the planner wants to design a containment policy that enables not-for-profit agents to break even at each period in the nursing homes service market. We formalize the planner's problem as an optimal control problem that combines a two-sector continuous-time individual-based mean-field epidemiological model and a production environment.

Our analysis reveals that each feasible solution to the planner's problem depends on the lockdown effectiveness, the infection incidence level tolerated by the social planner, the prevailing network of physical interactions that characterize the population, and exogenous epidemiological parameters. Using calibration that relies on parameters from the U.S. long-term care market, we show that the optimal lockdown decreases with lockdown effectiveness for not-for-profit nursing homes. However, the relationship between optimal lockdown policy and lockdown effectiveness for for-profit nursing homes is ambiguous. For an in-depth exploration of such association and its effect on COVID-19 fatalities, we turn to simulation and empirical analysis.

Using unique data on U.S. nursing home networks, as well as other data sources, we calibrate our mean-field network-based epidemiological model and jointly estimate the lockdown effectiveness (θ) and the tolerable COVID-19 infection incidence level (ι) for 40 U.S. states. Our estimated values show significant variations in these variables across U.S. states. We attribute some of these variations to state-level heterogeneity in economic and political factors and policy responses during the COVID-19 pandemic. Regression-based analyses show that for-profit nursing homes experience a higher death rate than not-for-profit nursing homes, and that this difference increases with lockdown effectiveness.

Appendix A Additional Figures

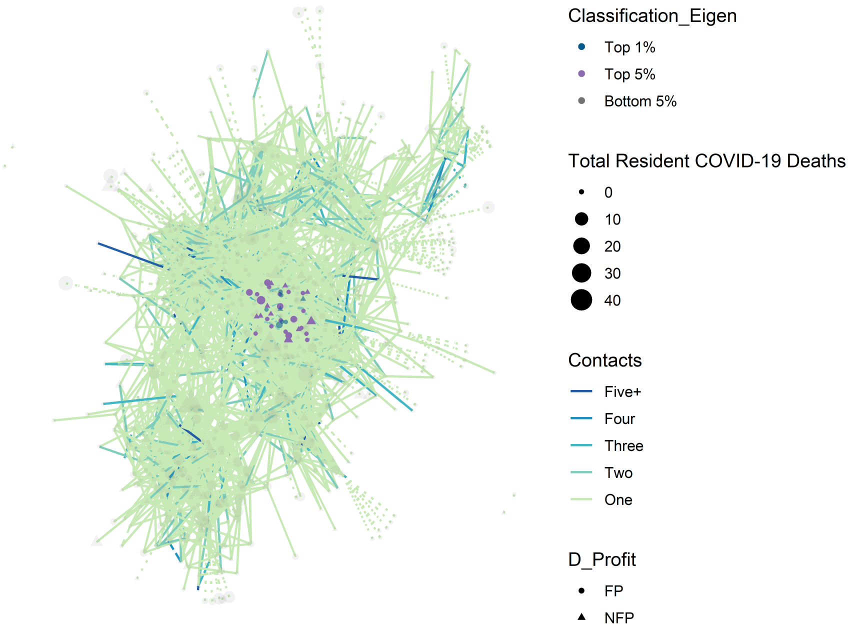

Fig. A1: Network structure for nursing homes in Florida with the eigenvector centrality measure. Notes: In the network, node size varies with the number of COVID-19 deaths among residents reported to the CMS as of May 31, 2020; shapes of nodes represent nursing homes' ownership, with the circle representing a FP nursing home, and a triangle representing a NFP nursing home; edge color differs with the number of contacts between nursing homes; a solid (resp. dotted) edge line corresponds to a connection between two nursing homes within the same U.S. state (resp. in two different states); and node color differences are based on eigenvector ranking, with the dark blue color, for example, highlighting the top 1% of facilities with high eigenvector centrality in the network.

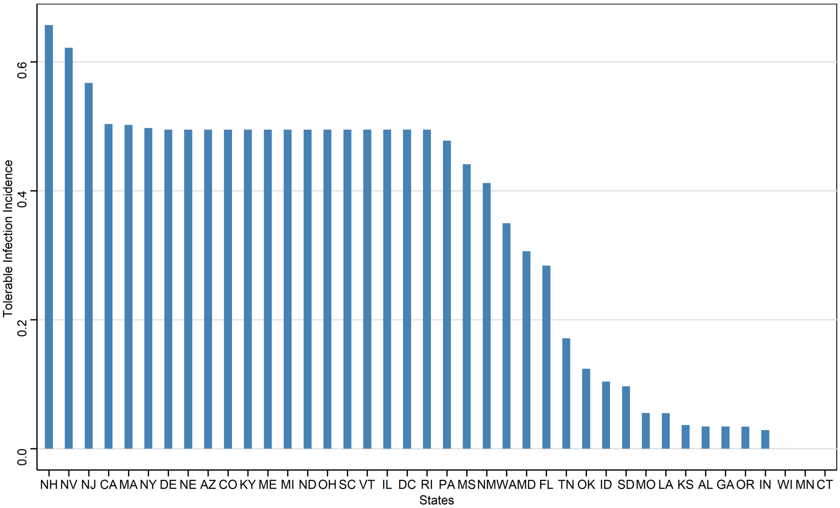

Fig. A2: Tolerable infection incidence across U.S. states (ι). Notes: The parameter ι estimates the tolerable COVID-19 infection incidence of the U.S. state governor from May 31 to August 16, 2020. Using the CMS data and the calibrated parameters in the model, we estimate ι for 40 U.S. states. The average value of estimates is 0.33 and the standard deviation is 0.22.

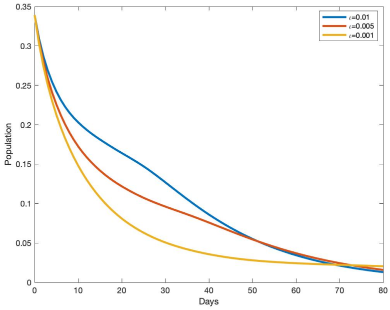

(a) Infection in FPs with $\theta = 0.9$

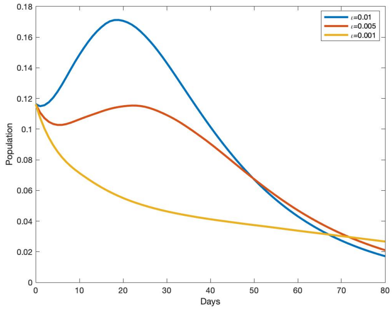

(b) Infection in NFPs with $\theta = 0.9$

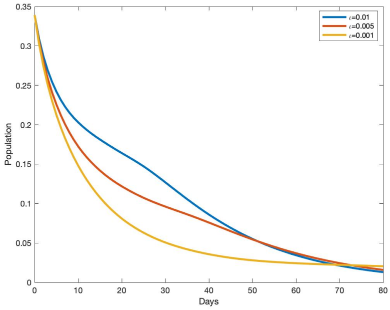

(c) Infection in FPs with $\theta = 0.5$

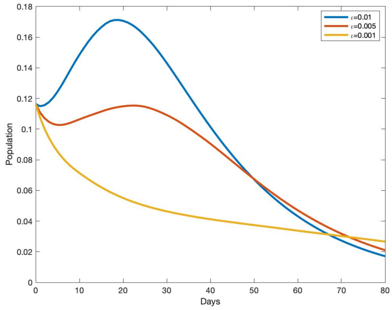

(d) Infection in NFPs with $\theta = 0.5$

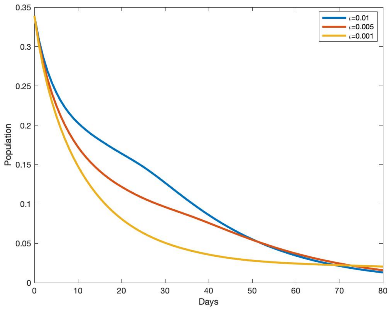

(e) Infection in FPs with $\theta = 0.35$

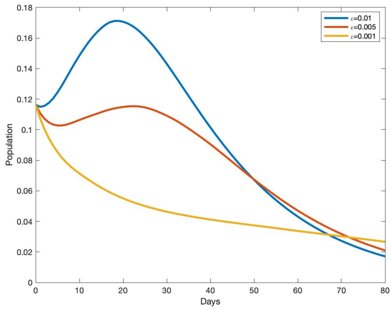

(f) Infection in NFPs with $\theta = 0.35$

Fig. A3: Infection and lockdown effectiveness in Florida.

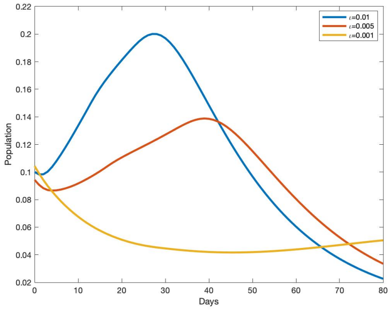

(a) Infection in FPs with $\theta = 0.9$

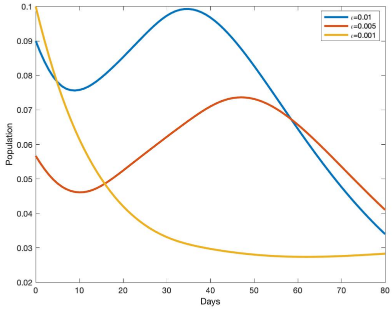

(b) Infection in NFPs with $\theta = 0.9$

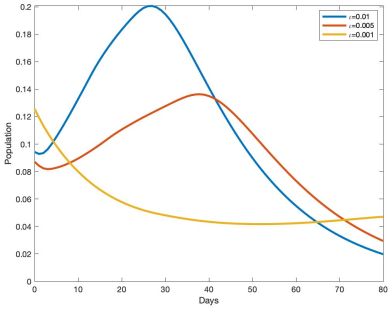

(c) Infection in FPs with $\theta = 0.5$

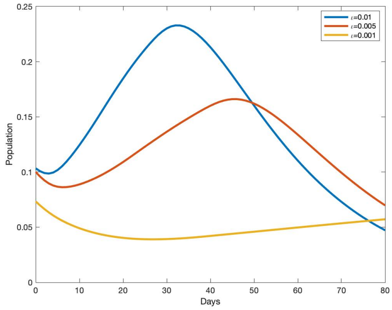

(d) Infection in NFPs with $\theta = 0.5$

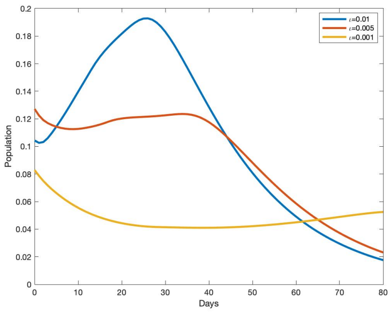

(e) Infection in FPs with $\theta = 0.1$

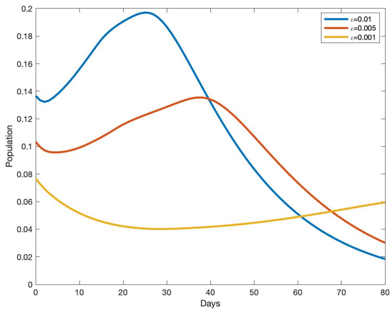

(f) Infection in NFPs with $\theta = 0.1$

Fig. A4: Infection and lockdown effectiveness in a random small-world network.

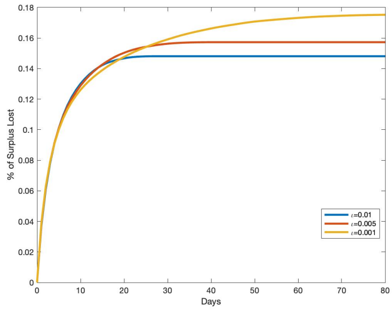

(a) Surplus lost in FPs with $\theta = 0.9$

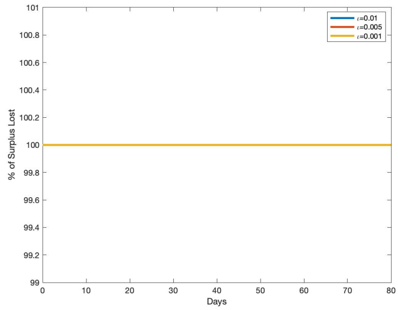

(b) Surplus lost in NFPs with $\theta = 0.9$

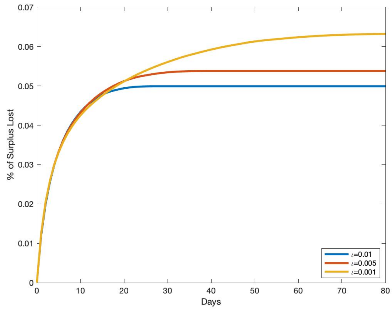

(c) Surplus lost in FPs with $\theta = 0.5$

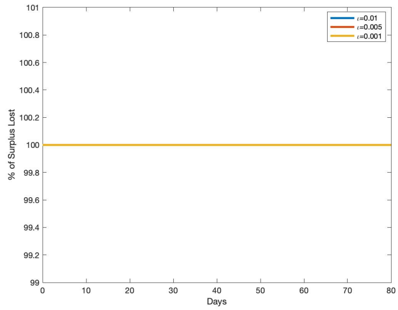

(d) Surplus lost in NFPs with $\theta = 0.5$

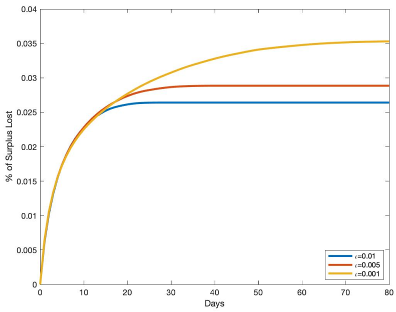

(e) Surplus lost in FPs with $\theta = 0.35$

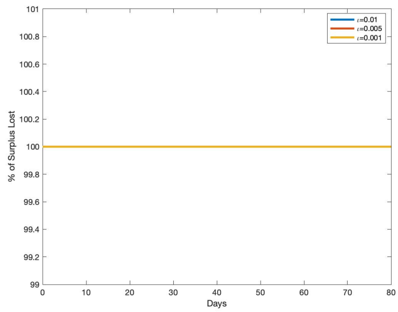

(f) Surplus lost in NFPs with $\theta = 0.35$

Fig. A5: Surplus lost dynamics and lockdown effectiveness in Florida.

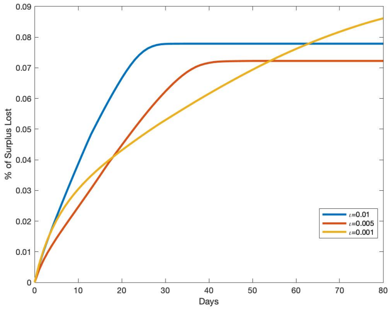

(a) Surplus lost in FPs with $\theta = 0.9$

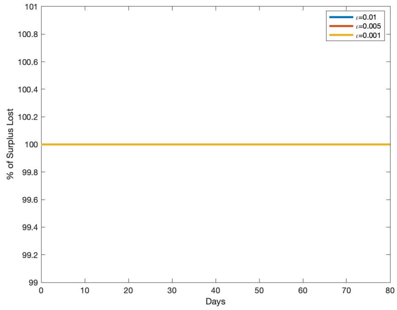

(b) Surplus lost in NFPs with $\theta = 0.9$

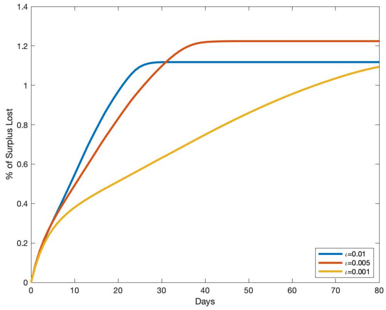

(c) Surplus lost in FPs with $\theta = 0.5$

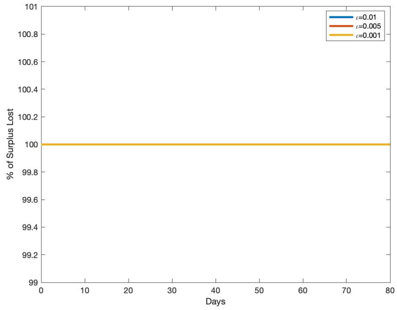

(d) Surplus lost in NFPs with $\theta = 0.5$

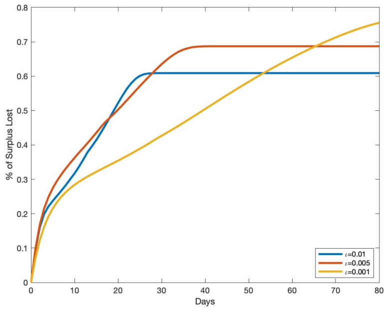

(e) Surplus lost in FPs with $\theta = 0.1$

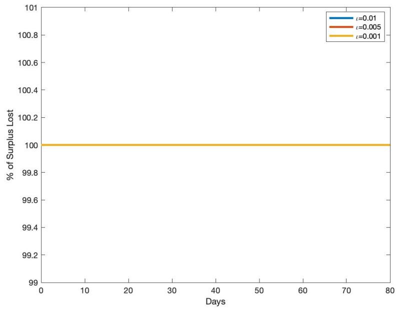

(f) Surplus lost in NFPs with $\theta = 0.1$

Fig. A6: Surplus lost dynamics and lockdown effectiveness in a random small-world network.

Appendix B Additional Tables

Table B1: Calibrated and estimated parameters sources and descriptions at U.S. state level

Parameters or Variables	Value	Definitions and Sources	Utilization
Epidemiological			
β	$\frac{R_0}{18}$	The COVID-19 reproduction numbers R_0 estimated during April to July 2020, from Statista	Calibration
γ	(1-death/case)/18	case and death per 1000 in nursing homes in each U.S. state as of Sep. 2020 from Statista	Calibration
κ	(death/case)/18	case and death per 1000 for in nursing homes in each U.S. state as of Sep. 2020 Statista	Calibration
Raw data Death Count	COVID-19 death	CMS data May 31 to August 16, 2020	Calibration
$\mathcal{M}$	Network of nursing homes	Protect Nursing Home Project	Calibration and Estimations
Economic			
For profit Indicator	Dummy variable indicating a nursing home's ownership (FP or NFP)	Replication data from Chen et al. (2021)	Calibration
Capital	Number of beds in the nursing home	Replication data from Chen et al. (2021)	Calibration
Price	Average hourly cost of a Private Room	Senior Living Project	Calibration
Wage	Average hourly wage by U.S. state	Bureau of Labor Statistics	Calibration
α	Cobb-Douglass production function	Replication data from Chen et al. (2021) and authors' estimations for each U.S state	Calibration
Regressions Tables	Variables	Replication data from Chen et al. (2021) and authors' calculations	Estimations

Table B2: Explaining θ with the OxCGRT indexes in U.S. states

	(Main)	(2)	(3)	(4)
ι	0.828***	0.662***	0.696***	0.681***
	(48.74)	(40.26)	(45.33)	(43.08)
Republican	-0.275***	-0.296***	-0.328***	-0.353***
	(-16.87)	(-18.98)	(-21.12)	(-23.02)
Governor Approval	0.0102***	0.00416***	0.00192***	0.00319***
	(34.34)	(15.03)	(5.86)	(10.31)
Economic Support Index	0.00365***	0.000255	0.000236	
	(17.72)	(1.22)	(1.23)	
D_Profit	-0.0873***	-0.0849***	-0.0966***	-0.100***
	(-11.08)	(-10.75)	(-12.72)	(-13.03)
Republican×D_Profit	0.0949***	0.0765***	0.0785***	0.0920***
	(8.67)	(7.57)	(7.53)	(8.78)
Covid_Death	-0.00244***	-0.00139***	-0.00206***	-0.00226***
	(-4.14)	(-2.69)	(-3.88)	(-4.14)
Covid_Death×D_Profit	0.00277***	0.00244***	0.00281***	0.00288***
	(4.02)	(4.05)	(4.59)	(4.58)
Republican×Covid_Death	0.00213***	0.00150**	0.00215***	0.00193***
	(2.76)	(2.53)	(3.35)	(2.93)
South	-0.251***	-0.317***	-0.299***	-0.281***
	(-26.52)	(-27.63)	(-26.90)	(-27.43)
Republican×South	0.312***	0.253***	0.223***	0.205***
	(24.48)	(19.71)	(16.85)	(16.66)
GDP_Growth	-0.0143***	-0.0102***	-0.00305	0.000422
	(-5.78)	(-4.26)	(-1.38)	(0.19)
Republican×GDP_Growth	-0.0138***	-0.0415***	-0.0455***	-0.0543***
	(-3.52)	(-11.42)	(-13.02)	(-16.31)
Stringency Index		0.0197***		
		(40.70)		
Containment Health Index			0.0224***	
			(46.27)	
Government Response Index				0.0212***
				(45.60)
Constant	-0.437***	-1.044***	-1.017***	-1.005***
	(-20.84)	(-42.76)	(-41.97)	(-41.13)
Observations	11535	11535	11535	11535
R^2	0.558	0.622	0.620	0.615

Notes: Data are from the CMS as of May 31, 2020, Chen et al. (2021), Hale et al. (2021), the COVID STATES PROJECT, and authors' estimations. The dependent variable is the estimated value of θ at the U.S. state. t statistics in parentheses. The first column title "Main" is the last column of Table 6. $^{*}p < 0.1$, $^{**}p < 0.05$, $^{***}p < 0.01$.

Table B3: Estimating the effects of lockdown effectiveness and other OxCGRT indexes on COVID-19 deaths in U.S. nursing homes

	(Main_Death)	(2)	(3)	(4)	(5)	(6)
θ	0.654***	0.321*	0.451***	0.211	0.574***	0.242
	(3.51)	(1.76)	(2.58)	(1.13)	(3.06)	(1.30)
D_Profit	-0.668***	-0.792***	-0.574***	-0.771***	-0.528***	-0.681***
	(-4.09)	(-4.83)	(-3.58)	(-4.75)	(-3.27)	(-4.15)
Eig_Cent	2.663***	2.412***	2.598***	2.384***	2.641***	2.453***
	(4.18)	(3.84)	(4.15)	(3.82)	(4.22)	(3.93)
Overall Rating	-0.168***	-0.166***	-0.164***	-0.165***	-0.165***	-0.163***
	(-3.83)	(-3.81)	(-3.75)	(-3.77)	(-3.76)	(-3.74)
County_ses	0.00792***	0.00743***	0.00644***	0.00699***	0.00629***	0.00651***
	(6.66)	(6.35)	(5.86)	(6.11)	(5.73)	(5.90)
$\theta\times$ D_Profit	1.919***	2.070***	1.751***	2.032***	1.678***	1.899***
	(6.49)	(7.00)	(6.06)	(6.95)	(5.73)	(6.43)
$\theta\times$ Eig_Cent	2.384*	2.886**	2.466**	2.915**	2.398**	2.754**
	(1.94)	(2.37)	(2.05)	(2.40)	(2.00)	(2.29)
$\theta\times$ County_ses	-0.000403	0.000146	-0.000799*	0.0000283	-0.000938**	-0.000366
	(-0.98)	(0.35)	(-1.94)	(0.07)	(-2.23)	(-0.84)
Governor Approval	0.0760***	0.0607***	0.0858***	0.0637***	0.0894***	0.0741***
	(10.23)	(8.11)	(11.34)	(8.52)	(11.93)	(9.97)
Stringency Index	0.0292***				-0.0187**	
	(3.45)				(-2.27)	
Containment Health Index		0.0849***				0.0446***
		(6.77)				(3.62)
Economic Support Index			0.0361***		0.0403***	0.0277***
			(6.93)		(7.11)	(5.11)
Government Response Index				0.0905***		
				(7.33)		
Constant	-3.937***	-6.349***	-5.128***	-6.927***	-4.492***	-6.550***
	(-4.94)	(-7.06)	(-6.92)	(-7.54)	(-5.51)	(-7.23)
County FE	Yes	Yes	Yes	Yes	Yes	Yes
Observations	11406	11406	11406	11406	11406	11406
R^2	0.088	0.091	0.092	0.092	0.092	0.093

Notes: Data are from the CMS as of May 31, 2020, Chen et al. (2021), Hale et al. (2021), and authors' estimations. The dependent variable is the number of COVID-19 deaths in a nursing home. The first column title "Main_Death" is the last column of Table 6. t statistics in parentheses. $^{*}p < 0.1$, $^{**}p < 0.05$, $^{***}p < 0.01$.

Table B4: Estimating the effects of lockdown effectiveness and other OxCGRT indexes on COVID-19 deaths in nursing homes in U.S. states with less effective lockdown strategies

	(1)	(2)	(3)	(4)	(5)	(6)
θ	-0.235	-0.261	-0.384*	-0.326	-0.385*	-0.401*
	(-1.09)	(-1.18)	(-1.83)	(-1.48)	(-1.84)	(-1.87)
D_Profit	0.226	0.171	0.241	0.153	0.236	0.210
	(1.05)	(0.79)	(1.13)	(0.71)	(1.11)	(0.97)
Eig_Cent	1.254*	1.195*	1.204*	1.154	1.200*	1.171*
	(1.77)	(1.68)	(1.70)	(1.63)	(1.70)	(1.66)
Overall Rating	-0.179***	-0.180***	-0.177***	-0.177***	-0.176***	-0.176***
	(-4.71)	(-4.73)	(-4.67)	(-4.68)	(-4.65)	(-4.64)
County_ses	0.000369	0.000586	0.00122	0.000859	0.00119	0.00126
	(0.38)	(0.60)	(1.25)	(0.88)	(1.21)	(1.29)
$\theta\times$ D_Profit	-0.419	-0.306	-0.400	-0.265	-0.396	-0.345
	(-1.00)	(-0.73)	(-0.96)	(-0.63)	(-0.95)	(-0.82)
$\theta\times$ Eig_Cent	1.595	1.699	1.653	1.753	1.657	1.705
	(0.98)	(1.04)	(1.01)	(1.08)	(1.02)	(1.05)
$\theta\times$ County_ses	-0.000341	-0.000346	-0.00116**	-0.000400	-0.00107*	-0.000986*
	(-0.64)	(-0.67)	(-2.37)	(-0.79)	(-1.88)	(-1.88)
Governor Approval	0.0610***	0.0610***	0.0617***	0.0568***	0.0601***	0.0584***
	(5.25)	(5.60)	(5.92)	(5.14)	(5.18)	(5.31)
Stringency Index	0.0181**				0.00370	
	(2.13)				(0.36)	
Containment Health Index		0.0244**				0.00992
		(2.15)				(0.78)
Economic Support Index			0.0172***		0.0164***	0.0159***
			(4.01)		(3.16)	(3.31)
Government Response Index				0.0334***		
				(3.15)		
Constant	-2.750***	-3.051***	-2.845***	-3.372***	-2.926***	-3.137***
	(-3.93)	(-4.02)	(-4.10)	(-4.59)	(-4.23)	(-4.16)
County FE	Yes	Yes	Yes	Yes	Yes	Yes
Observations	5169	5169	5169	5169	5169	5169
R^2	0.128	0.128	0.130	0.129	0.130	0.130

Notes: Data are from the CMS as of May 31, 2020, Chen et al. (2021), Hale et al. (2021), and authors' estimations. The dependent variable is the number of COVID-19 deaths in a nursing home. t statistics in parentheses. $^{*}p < 0.1$, $^{**}p < 0.05$, $^{***}p < 0.01$.

Table B5: Estimating the effects of lockdown effectiveness and other OxCGRT indexes on COVID-19 deaths in nursing homes in U.S. states with highly effective lockdown strategies

	(1)	(2)	(3)	(4)	(5)	(6)
θ	7.804***	6.947***	2.833	5.372***	3.848*	4.386**
	(3.88)	(3.50)	(1.44)	(2.73)	(1.95)	(2.22)
D_Profit	-0.699***	-0.745***	-0.693***	-0.811***	-0.488**	-0.481**
	(-2.84)	(-3.02)	(-2.92)	(-3.31)	(-2.02)	(-1.97)
Eig_Cent	2.968***	2.922***	2.616**	2.816**	2.725**	2.702**
	(2.68)	(2.64)	(2.38)	(2.54)	(2.49)	(2.46)
Overall Rating	-0.167**	-0.167**	-0.163**	-0.168**	-0.159**	-0.159**
	(-2.30)	(-2.30)	(-2.25)	(-2.31)	(-2.19)	(-2.19)
County_ses	0.0137***	0.0131***	0.00577**	0.0116***	0.00489**	0.00502**
	(6.34)	(5.85)	(2.41)	(5.05)	(2.05)	(2.13)
$\theta\times$ D_Profit	2.530***	2.551***	2.321***	2.586***	1.995***	2.077***
	(5.94)	(6.09)	(5.79)	(6.24)	(4.91)	(5.14)
$\theta\times$ Eig_Cent	3.576*	3.715**	4.405**	3.979**	4.203**	4.143**
	(1.91)	(1.99)	(2.36)	(2.12)	(2.28)	(2.24)
$\theta\times$ County_ses	-0.00105	-0.000759	0.00000434	-0.000348	-0.000169	-0.000607
	(-1.58)	(-1.11)	(0.01)	(-0.51)	(-0.26)	(-0.92)
Government Approval	0.0930***	0.0873***	0.140***	0.0890***	0.147***	0.169***
	(7.96)	(7.99)	(8.88)	(7.97)	(9.58)	(10.22)
Stringency Index	0.0110				-0.0656***	
	(0.62)				(-4.14)	
Containment Health Index		0.0343				-0.0927***
		(1.58)				(-4.48)
Economic Support Index			0.0693***		0.0833***	0.0917***
			(5.26)		(6.14)	(6.21)
Government Response Index				0.0687***		
				(2.94)		
Constant	-9.979***	-10.41***	-12.94***	-11.52***	-10.86***	-11.61***
	(-3.93)	(-4.30)	(-5.29)	(-4.61)	(-4.23)	(-4.70)
County FE	Yes	Yes	Yes	Yes	Yes	Yes
Observations	6237	6237	6237	6237	6237	6237
R^2	0.094	0.094	0.099	0.095	0.100	0.101

Notes: Data are from the CMS as of May 31, 2020, Chen et al. (2021), Hale et al. (2021), and authors' estimations. The dependent variable is the number of COVID-19 deaths in a nursing home. t statistics in parentheses. $^{*}p < 0.1$, $^{**}p < 0.05$, $^{***}p < 0.01$.

References

Acemoglu, D., Chernozhukov, V., Werning, I., Whinston, M.D. (2021). Optimal targeted lockdowns in a multigroup SIR model. *American Economic Review: Insights*, *3*(4), 487–502.

Akhtar-Danesh, N., Baumann, A., Crea-Arsenio, M., Antonipillai, V. (2022). Covid-19 excess mortality among long-term care residents in Ontario, Canada. *Plos One*, *17*(1), e0262807.

Alvarez, F.E., Argente, D., Lippi, F. (2021). A simple planning problem for COVID-19 lock-down, testing, and tracing. *American Economic Review: Insights*, *3*(3).

Assob-Nguedia, J.-C., Dongo, D., Nguimkeu, P.E. (2020). Early dynamics of transmission and projections of COVID-19 in some west african countries. *Infectious Disease Modelling*, *5*, 839–847.

Baccini, L., & Brodeur, A. (2021). Explaining governors' response to the COVID-19 pandemic in the United States. *American Politics Research*, *49*(2), 215–220.

Bach-Mortensen, A.M., Verboom, B., Movsisyan, A., Degli Esposti, M. (2021). A systematic review of the associations between care home ownership and covid-19 outbreaks, infections and mortality. *Nature Aging*, *1*(10), 948–961.

Ballester, C., Calvó-Armengol, A., Zenou, Y. (2006). Who's who in networks. wanted: The key player. *Econometrica*, *74*(5), 1403–1417.

Banerjee, A., Chandrasekhar, A.G., Duflo, E., Jackson, M.O. (2013). The diffusion of microfinance. *Science*, *341*(6144).

Battiston, P., & Stanca, L. (2015). Boundedly rational opinion dynamics in social networks: Does indegree matter? *Journal of Economic Behavior & Organization*, *119*, 400–421.

Boucekkine, R., Carvajal, A., Chakraborty, S., Goenka, A. (2021). The economics of epidemics and contagious diseases: An introduction. *Journal of Mathematical Economics*, *93*, 102498.

Buechel, B., Hellmann, T., Klößner, S. (2015). Opinion dynamics and wisdom under conformity. *Journal of Economic Dynamics and Control*, *52*, 240–257.

Chen, M.K., Chevalier, J.A., Long, E.F. (2021). Nursing home staff networks and COVID-19. *Proceedings of the National Academy of Sciences*, *118*(1).

Comas-Herrera, A., Zalakaín, J., Lemmon, E., Henderson, D., Litwin, C., Hsu, A.T., ... Fernández, J.-L. (2020). Mortality associated with covid-19 in care homes: international evidence. *Article in LTCcovid.org, international long-term care policy network, CPEC-LSE*, *14*.

Conlen, M., Ivory, D., Yourish, K., Lai, R., Hassan, A., Calderone, J. (2021). *Nearly one-third of U.S. coronavirus deaths are linked to nursing homes.* (Accessed at https://www.nytimes.com/interactive/2020/us/coronavirus-nursing-homes.html)

Debnam Guzman, J., Mabeu, M.C., Pongou, R. (2022). Identity during a crisis: COVID-19 and ethnic divisions in the United States. *AEA Papers and Proceedings*, *112*, 319-–324.

Dessie, Z.G., & Zewotir, T. (2021). Mortality-related risk factors of COVID-19: a systematic review and meta-analysis of 42 studies and 423,117 patients. *BMC Infectious Diseases*, *21*(1), 1–28.

Dykgraaf, S.H., Matenge, S., Desborough, J., Sturgiss, E., Dut, G., Roberts, L., ... Kidd, M. (2021). Protecting nursing homes and long-term care facilities from covid-19: a rapid review of international evidence. *Journal of the American Medical Directors Association*, *22*(10), 1969–1988.

Fajgelbaum, P.D., Khandelwal, A., Kim, W., Mantovani, C., Schaal, E. (2021). Optimal lockdown in a commuting network. *American Economic Review: Insights*, *3*(4), 503–22.

Fallon, A., Dukelow, T., Kennelly, S.P., O'Neill, D. (2020). Covid-19 in nursing homes. *QJM: An International Journal of Medicine*, 391–392.

Favreault, M.M., & Johnson, R.W. (2021). Projections of risk of needing long-term services and supports at ages 65 and older. *Washington DC: US Department of Health and Human Services, Office of the Assistant Secretary for Planning and Evaluation.*

Forneron, J.-J., & Ng, S. (2018). The ABC of simulation estimation with auxiliary statistics. *Journal of Econometrics*, *205*(1), 112–139.

Galeotti, A., Golub, B., Goyal, S. (2020). Targeting interventions in networks. *Econometrica*, *88*(6), 2445–2471.

Gertler, P.J., & Waldman, D.M. (1992). Quality-adjusted cost functions and policy evaluation in the nursing home industry. *Journal of Political Economy*, *100*(6), 1232–1256.

Giri, S., Chenn, L.M., Romero-Ortuno, R. (2021). Nursing homes during the COVID-19 pandemic: a scoping review of challenges and responses. *European Geriatric Medicine*, *12*(6), 1127–1136.

Gollier, C. (2020). Cost–benefit analysis of age-specific deconfinement strategies. *Journal of Public Economic Theory*, *22*(6), 1746–1771.

Hale, T., Angrist, N., Goldszmidt, R., Kira, B., Petherick, A., Phillips, T., … Tatlow, H. (2021). A global panel database of pandemic policies (Oxford COVID-19 Government Response Tracker). *Nature Human Behaviour*, *5*(4), 529–538.

Ioannidis, J.P., Axfors, C., Contopoulos-Ioannidis, D.G. (2021). Second versus first wave of COVID-19 deaths: shifts in age distribution and in nursing home fatalities. *Environmental Research*, *195*, 110856.

JCHS (2016). *Implications for housing a growing population: Older households 2015–2035.* (Accessed at https://www.jchs.harvard.edu/sites/default/files/harvard_jchs_housing_growing_population_2016.pdf)

Lloyd, A.L., Valeika, S., Cintrón-Arias, A. (2006). Infection dynamics on small-world networks. *Contemporary Mathematics*, *410*, 209–234.

Makris, M. (2021). Covid and social distancing with a heterogenous population. *Economic Theory*, 1–50.

Neelon, B., Mutiso, F., Mueller, N.T., Pearce, J.L., Benjamin-Neelon, S.E. (2021). Associations between governor political affiliation and COVID-19 cases, deaths, and testing in the US. *American Journal of Preventive Medicine*, *61*(1), 115–119.

Nganmeni, Z., Pongou, R., Tchantcho, B., Tondji, J.-B. (2022). Vaccine and inclusion. *Journal of Public Economic Theory*, *Forthcoming*.

Nguimkeu, P. (2014). A structural econometric analysis of the informal sector heterogeneity. *Journal of Development Economics*, *107*, 175–191.

Nguimkeu, P., & Okou, C. (2021). Does informality increase the spread of covid-19 in africa? a cross-country examination. *Applied Economics Letters*, 1–5.

Nguimkeu, P., & Tadadjeu, S. (2021). Why is the number of COVID-19 cases lower than expected in Sub-Saharan Africa? a cross-sectional analysis of the role of demographic and geographic factors. *World Development*, *138*, 105251.

O'Neill, D., Briggs, R., Holmerová, I., Samuelsson, O., Gordon, A.L., Martin, F.C. (2020). Covid-19 highlights the need for universal adoption of standards of medical care for physicians in nursing homes in Europe. *European Geriatric Medicine*, *11*(4), 645–650.

Pastor-Satorras, R., Castellano, C., Van Mieghem, P., Vespignani, A. (2015). Epidemic processes in complex networks. *Reviews of Modern Physics*, *87*(3), 925.

Pongou, R., & Serrano, R. (2013). Fidelity networks and long-run trends in HIV/AIDS gender gaps. *American Economic Review*, *103*(3), 298–302.

Pongou, R., Tchuente, G., Tondji, J.-B. (2022a). Laissez-faire, social networks, and race in a pandemic. *AEA Papers and Proceedings*, *112*, 325—329.

Pongou, R., Tchuente, G., Tondji, J.-B. (2022b). Optimal Interventions in Networks during a Pandemic. *Journal of Population Economics*, *Forthcoming*.

Pongou, R., & Tondji, J.-B. (2018). Valuing inputs under supply uncertainty: The bayesian Shapley value. *Games and Economic Behavior*, *108*, 206–224.

Watts, D.J., & Strogatz, S.H. (1998). Collective dynamics of 'small-world' networks. *Nature*, *393*(6684), 440–442.

WHO (2022). *WHO Coronavirus (COVID-19) Dashboard With Vaccination Data.* (Accessed at https://covid19.who.int/)

Young, H.P. (2009). Innovation diffusion in heterogeneous populations: Contagion, social influence, and social learning. *American Economic Review*, *99*(5), 1899–1924.

Young, H.P. (2011). The dynamics of social innovation. *Proceedings of the National Academy of Sciences*, *108*(Supplement 4), 21285–21291.